

5-25-2017

DNA Mismatch Repair Dependent Damage Response in Human Pluripotent Stem Cells and Intestinal Organoids

Bo Lin
bolin@uchc.edu

Follow this and additional works at: <https://opencommons.uconn.edu/dissertations>

Recommended Citation

Lin, Bo, "DNA Mismatch Repair Dependent Damage Response in Human Pluripotent Stem Cells and Intestinal Organoids" (2017).
Doctoral Dissertations. 1535.
<https://opencommons.uconn.edu/dissertations/1535>

DNA Mismatch Repair Dependent Damage Response in Human Pluripotent Stem Cells and Intestinal Organoids

Bo Lin, Ph.D.

University of Connecticut, 2017

The DNA mismatch repair (MMR) pathway is a very important DNA repair pathway to maintain genomic integrity. Germline mutations in the MMR genes can cause a hereditary cancer predisposition syndrome, Lynch Syndrome (LS). LS patients develop colorectal cancer as well as other extracolonic cancers at an early age. However, how the loss of DNA MMR leads to tumorigenesis remains unclear. The MMR mediated DNA damage response to the alkylating agent *N*-methyl-*N*'-nitro-*N*-nitrosoguanidine (MNNG) observed in various cancer cell lines may contribute to preventing tumorigenesis by eliminating damaged cells. In the first part of this study, we examined the MMR dependent DNA damage response in the human pluripotent stem cell (hPSC) which is a nontransformed cell model. We found that hPSCs are hypersensitive to alkylation damage which triggers massive apoptosis. Interestingly, the nature of this alkylation response differs from that previously reported in somatic cells. In somatic cells, a permanent G₂/M cell cycle arrest is induced in the second cell cycle after DNA damage. The hPSCs, however, directly undergo apoptosis in the first cell cycle. Furthermore, the signaling mechanisms of this damage response are also very different from somatic cells in that the checkpoint kinases Chk1 and Chk2 are not activated in hPSCs in response to alkylation damage, but rather p53 activation is responsible for

inducing apoptosis. This response reveals that hPSCs rely on apoptotic cell death as an important defense to avoid mutation accumulation.

Since LS patients predominantly develop colorectal cancer and human embryonic stem cells (hESCs) can be differentiated into intestinal organoids *in vitro*, in the second part of this study we generated both hESCs-derived human intestinal organoids (HIOs) and adult human intestinal enteroids (HIEs) from patient colon samples to study the damage responses to alkylation damage in intestinal cells specifically. We found that the MMR pathway can direct multiple responses to DNA damage in different intestinal cell types in HIOs. Intestinal stem cells (ISCs) appear more prone to undergo apoptosis in response to DNA damage whereas more differentiated cells such as the transient amplifying cells are more likely to senesce. Both mechanisms may play an important role in tumor suppression by eliminating or halting progression of damaged cells. Therefore loss of MMR pathway function might provide an immediate selective advantage at an early stage during tumorigenesis in LS patients. Taken together, this work further reveals the MMR-dependent DNA damage response in nontransformed cell types and cell types related to LS, and provides insights into how loss of these damage responses may contribute to tumorigenesis at an early stage in LS patients.

DNA Mismatch Repair Dependent Damage Response in Human Pluripotent Stem Cells
and Intestinal Organoids

Bo Lin

M.B. Southeast University, 2011

A Dissertation

Submitted in Partial Fulfillment of the

Requirements of the Degree of

Doctor of Philosophy

at the

University of Connecticut

2017

APPROVAL PAGE

Doctor of Philosophy Dissertation

DNA Mismatch Repair Dependent Damage Response in Human Pluripotent Stem Cells
and Intestinal Organoids

Presented by

Bo Lin, M.B.

Major Advisor _____
Christopher D. Heinen

Associate Advisor _____
Sandra K. Weller

Associate Advisor _____
Ann Cowan

Associate Advisor _____
Stormy J. Chamberlain

University of Connecticut

2017

ACKNOWLEDGEMENTS

My graduate education has been a challenging but inspirational experience for me. There are many people who have supported and helped me in this adventure.

Foremost, my mentor, Dr. Christopher Heinen. Thank you for your many years of advice and guidance filled with encouragement. You have always made time for me and provided me many opportunities to explore new areas to grow. Your mentoring has been inspiring with tremendous support. I always feel very lucky to do my PhD in your lab because you are really devoted to the graduate students beyond research in the lab. I have been grateful for your support of me pursuing my next step in career as a resident in pathology.

I would also like to thank my committee members: Dr. Sandra Weller for many helpful discussions and guidance, Dr. Ann Cowan for teaching me the microscopy skills and advising me over the years and Dr. Stormy Chamberlain for training me all the stem cell techniques and helping me get started with the pluripotent stem cell project.

To all the past and present members of the Heinen Lab, thank you for your support and making the lab a fun and relaxed place to work in. A special thank you to Dr. Jenifer Cyr, who taught me most of the lab techniques when I first joined the lab with minimum lab experience. Also special thanks to Dipika Gupta for being a great friend and all the years we have shared in the lab, going through struggles when experiments don't work and excitements in our progress and milestones. I would like to also thank our technician Qingfen Yang, who helped me a lot in my intestinal organoid project.

Importantly, I would like to thank all the members of the University of Connecticut Health community including the Molecular Biology and Biochemistry Graduate Program, the Center for Molecular Medicine and Dr. Iman Al-Naggar in the Center on Aging. Without their support this work would not have been possible.

A special thank you to Dr. Thomas Manger, Dr. Lynn Kosowicz and Dr. Qian Wu for giving me the opportunity to gain some clinical experience here. It has been very helpful for me to get into the residency program.

Finally, I must thank my family and friends for my accomplishment, even though many of them have been thousands of miles away from me. Without your love and support, I would never have come so far. Thank you.

TABLE OF CONTENTS

List of tables	viii
List of figures	ix
List of abbreviations	xi
Chapter 1: Introduction	
A. Lynch syndrome	1
B. Mismatch repair	3
C. Human pluripotent stem cells	9
D. Intestinal organoids	12
E. Senescence	15
Chapter 2: Human Pluripotent Stem Cells Have A Novel Mismatch Repair-Dependent Damage Response	
A. Abstract	16
B. Introduction	17
C. Materials and methods	21
D. Results	25
E. Discussion	49
Chapter 3: The Use of Human Intestinal Organoids to Study the Effects of Early Cancer-causing Mutations on Intestinal Stem Cells	
A. Abstract	56
B. Introduction	57
C. Materials and methods	58

D. Results	62
E. Discussion	82
 Chapter 4: Conclusions and Future Directions	
A. MMR- dependent DNA damage response in hPSCs	84
B.MMR- dependent DNA damage response in HIOs	87
 References	 92

LIST OF TABLES

<u>Table</u>	<u>Title</u>	<u>Page</u>
Table 1-1	Amsterdam Criteria II	2
Table 3-1	Antibodies used for immunofluorescence staining	80
Table 3-2	RT-PCR primers	81

LIST OF FIGURES

<u>Figure</u>	<u>Title</u>	<u>Page</u>
Figure 1-1	Mechanism of mismatch repair	5
Figure 1-2	Proposed models for activation of the MMR-dependent DNA damage response	10
Figure 1-3	Architecture of the colon crypt	13
Figure 2-1	Human pluripotent stem cells express higher levels of MMR proteins than parental fibroblasts	26
Figure 2-2	Human pluripotent stem cells repair mismatches more efficiently than parental fibroblasts	29
Figure 2-3	DNA alkylation damage induces apoptosis in human pluripotent stem cells	32
Figure 2-4	The apoptotic response to alkylation damage in induced pluripotent stem cells is mismatch repair dependent	35
Figure 2-5	MNNG-induced apoptosis occurs in a mismatch repair-dependent manner in the first S-phase after damage	38
Figure 2-6	Pluripotent stem cells that survive MNNG treatment retain sensitivity to MNNG	41
Figure 2-7	Chk1 and Chk2 are not activated in induced pluripotent stem cells in response to MNNG, but p53 is	44
Figure 2-8	MNNG treatment leads to phosphorylation of ATR and ATM in pluripotent stem cells	47
Figure 2-9	Model of the mismatch repair-dependent damage response to alkylation damage in somatic cells versus human	53

	pluripotent stem cells	
Figure 3-1	Generation of HIOs from hESCs	64
Figure 3-2	MSH2 expression and knockout in HIOs	66
Figure 3-3	Alkylation damage leads to both a MMR-dependent apoptotic and senescent response	70
Figure 3-4	The MMR-dependent apoptotic response to damage occurs primarily in intestinal stem cells	73
Figure 3-5	Adult human intestinal enteroids display both apoptotic and senescent responses to alkylation damage	77
Figure 3-S1	Cell survival of hESCs after MNNG treatment	79
Figure 4-1	MMR deficient ISCs gain survival advantage to populate crypts	90

LIST OF ABBREVIATIONS

5-FU	5-fluorouracil
ATM	Ataxia-telangiectasia mutated
ATR	Ataxia telangiectasia and Rad3-related protein
BER	Base excision repair
BG	Benzylguanine
CRC	Colorectal cancer
ESCs	Embryonic stem cells
hESCs	Human embryonic stem cells
HIOs	Human intestinal organoids
HIEs	Human intestinal enteroids
HRR	Homologous recombination repair
hPSCs	Human pluripotent stem cells
IDLs	Insertion/deletion loops
iPSCs	Induced pluripotent stem cells
IR	Gamma-irradiation
ISCs	Intestinal stem cells
KO	Knockout
LS	Lynch syndrome
MeG	Methylguanine
MMR	Mismatch repair
MNNG	<i>N</i> -methyl- <i>N</i> -nitro- <i>N</i> -nitrosoguanidine
MSI	Microsatellite instability
PCNA	Proliferating cell nuclear antigen
PI	Propidium iodide
PIKK	Phosphatidylinositol 3-kinase-related kinase
PSCs	Pluripotent stem cells
SASP	Senescence associated secretory phenotype
SSBP	Single-strand binding protein
ssDNA	Single-strand DNA
TA	Transient amplifying
UV	ultra-violet

CHAPTER 1

Introduction

A. Lynch Syndrome

Lynch Syndrome (LS) is a hereditary cancer syndrome that predisposes patients to colorectal cancer as well as other extracolonic cancers including endometrial cancer, ovarian cancer, gastric cancer etc. It is the most common form of hereditary colon cancer, accounting for approximately 2-7% of all colorectal cancers. These cancers are typically early onset, rapidly progressing and resistant to many chemotherapeutic agents. Lynch syndrome is caused by mutations in DNA mismatch repair (MMR) genes (*MSH2*, *MSH6*, *MLH1*, *PMS2*) and inherited in an autosomal dominant fashion. An individual inherits one defective allele and loses the remaining wild type copy sporadically later during their lifetime (Poulogiannis et al., 2010; Lynch et al., 2015). The diagnosis is now based on genetic testing of MMR genes. The revised Amsterdam criteria II guidelines have been used clinically to identify high-risk candidates for genetic testing and rely heavily on family history (Table 1-1) (Vasen et al., 2007). Due to limitations of the Amsterdam criteria, many patients were likely missed so now many medical centers perform molecular testing on all colorectal cancer (CRC) patients, including test for microsatellite instability which is a hallmark of MMR deficiency and immunohistochemistry for MMR proteins prior to sequencing for MMR mutations. Identified carriers of MMR mutations are advised to undergo early and frequent cancer screenings as well as preventive surgeries. Once a tumor is detected, the first line

Table 1-1 Amsterdam Criteria II for Lynch syndrome

1. Three or more relatives with an LS-associated cancer (colorectal cancer, endometrial cancer, cancer of the small bowel, ureter or renal pelvis), one of whom is a first-degree relative of the other two.
2. At least two successive generations affected
3. At least one case diagnosed before age 50
4. Familial adenomatous polyposis excluded
5. Tumors verified by pathologic examination

therapy is surgery and chemotherapy. However, LS tumors are naturally resistant to the commonly used chemotherapeutic agent for colorectal cancer 5-fluorouracil (5-FU) due to MMR deficiency, highlighting the need for novel therapeutics for LS patients (Tajima et al., 2004).

B. Mismatch repair

DNA MMR is a highly conserved cellular process throughout evolution and is essential for maintaining genomic integrity. MMR can recognize and repair base mismatches and small insertion/deletion loops (IDLs) that arise in DNA primarily due to polymerase misincorporation errors, but also through cellular and exogenous DNA damaging agents (Jiricny, 2006) (Li, 2008). The mechanism of MMR has been extensively studied in *Escherichia coli* and repair by the bacterial system has been reconstituted *in vitro*. This purified system relies on the activities of the MMR proteins MutS, MutL, and MutH, as well as DNA helicase II, exonuclease I, single-strand binding protein (SSBP), DNA polymerase III, and DNA ligase (Lahue et al., 1989). The MMR system is evolutionarily conserved from bacteria to humans, though MMR in the eukaryotic system is more complex. Several MutS and MutL homologs have been identified in the yeast and mammalian systems (Fishel and Wilson, 1997). MutS homologs MSH2, MSH3, and MSH6 form two heterodimeric complexes with specific yet partially redundant DNA lesion recognition activities. MSH2-MSH6 recognizes single base-base mismatches and small IDL loops in DNA, while MSH2-MSH3 primarily recognizes larger IDL loops. MSH2-MSH6 signals for repair through a heterodimer of MutL homologs MLH1-PMS2. In

addition to the activities of MSH2-MSH6 and MLH1-PMS2, this system requires exonuclease I, the SSBP RPA, polymerase δ , proliferating cell nuclear antigen (PCNA), the clamp loader RFC, and DNA ligase I (Constantin et al., 2005; Zhang et al., 2005). Briefly, a single basepair mismatch can be recognized by MSH2-MSH6, which will then recruit MLH1-PMS2 and exonuclease I leading to the excision of the erroneous strand. Finally, the resulting single stranded gap is filled in by polymerase resynthesis and ligated by DNA ligase I (Figure 1-1) (Martin and Scharff, 2002). *In vitro* experiments reveal that the excision requires that the heteroduplex substrate contains a pre-existing nick on the mismatch-containing strand as an entry site for exonuclease I and serves as a discrimination signal to distinguish the strand to be removed from the template. *In vivo*, this discrimination signal could come from gaps between Okazaki fragments in the lagging strand or the 3' terminus of the newly synthesized leading strand. How MLH1-PMS2 is able to detect these structural signals when they may be hundreds of bases away from the mismatch is unclear (Jiricny, 2006).

Loss of MMR gives rise to an elevated mutation rate, termed the mutator phenotype, as uncorrected DNA errors become permanent mutations during a subsequent round of DNA replication (Loeb et al., 1974). In MMR defective cells, the mutator phenotype manifests in a type of genomic instability called microsatellite instability (MSI). Mononucleotide, dinucleotide, and larger repeats in the genome are prone to template slipping during replication due to transient fluctuations in primer annealing. The resulting looped out bases are normally repaired by the DNA MMR system but become permanent insertions or deletions when MMR is not functioning. Thus, defective MMR is

Figure 1-1.

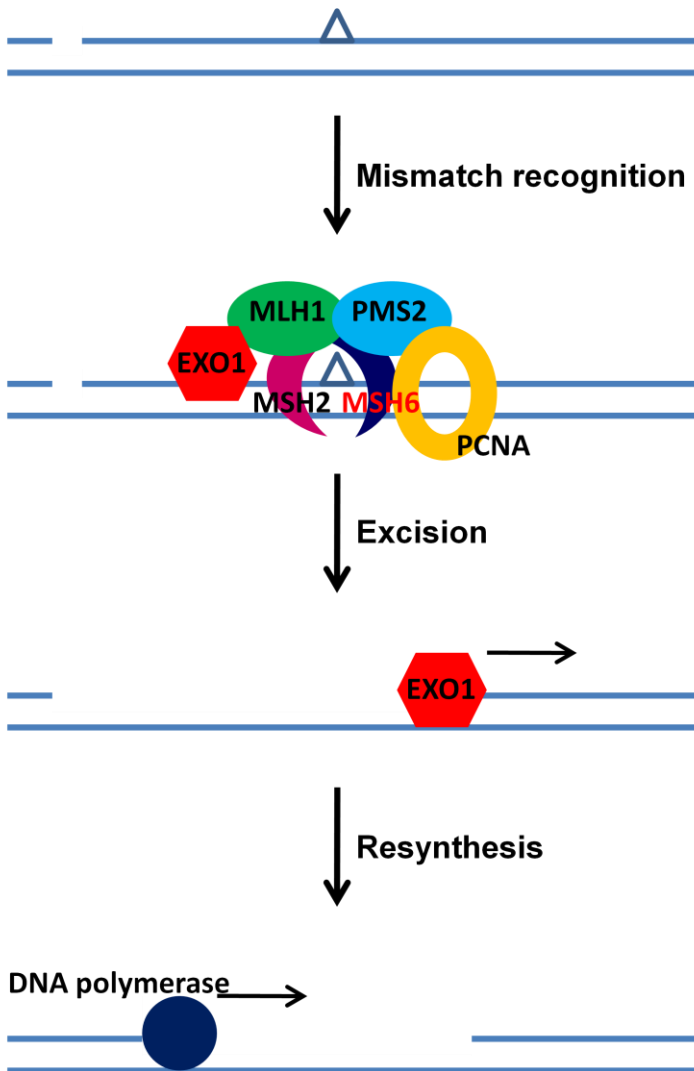


Figure 1-1.Mechanism of mismatch repair.

The MSH2–MSH6 heterodimer binds to single base-pair mismatches, which then recruits MLH1-PMS2 as well as the Exo1 exonuclease to the DNA. PCNA which links the DNA polymerase to the DNA template during replication, also interacts with this complex, indicating that MMR might be closely associated with the DNA replication fork (Harfe and Jinks-Robertson, 2000). Single-stranded DNA breaks occur during MMR, although it is unclear whether they are already present at the replication fork or caused by the endonuclease activity of MLH1-PMS2 or both. The mismatch-containing strand is excised by exonuclease Exo1 and then filled-in by DNA polymerase and ligated by DNA ligase I.

not thought to lead to a direct growth advantage as with classic tumor suppressor genes, but rather, due to the resultant mutator phenotype, it increases the likelihood that other tumor suppressor genes and oncogenes will become mutated. Several critical genes involved in cell growth and cell survival (for example TGF β RII, β -catenin, and BAX) are mutated more often in MMR deficient cells than in normal cells (Duval and Hamelin, 2002).

Besides the protection of genome stability, another MMR function maybe be involved in preventing tumorigenesis. We propose that the MMR-dependent DNA damage response may directly affect cell survival. The MMR pathway plays a vital role in the induction of cell cycle arrest and apoptosis in response to certain forms of DNA damage. The MSH2-MSH6heterodimer can recognize and bind to an array of lesions including the G/T mismatch, O⁶methyl-G/C, O⁶methyl-G/T, cisplatin adducts, and fluorinated pyrimidine lesions in DNA generated by 5-FU (Duckett et al., 1996; Hsieh and Yamane, 2008). Interestingly, MMR-deficiency confers tolerance to many DNA damaging agents that cause these DNA adducts (Stojic et al., 2004a). MMR-proficient human cell lines were demonstrated to be 100-fold more sensitive to alkylation damage than MMR deficient cells (Karran, 2001).The most well studied alkylating agent in relation to MMR mediated DNA damage response is MNNG, which acts as an Sn1 donor and targets the O⁶position of guanine to produce the cytotoxic O⁶-meG lesion (Gerson, 2004). The cell utilizes methylguanine methyltransferase (MGMT) to remove the methyl group in a reaction that inactivates MGMT but restores the unmodified guanine. However, if allowed to persist during DNA replication, the O⁶-meG can be mispaired with thymidine

to form O⁶-meG /T mismatches, which ultimately results in G/C to A/T transitions (Gerson, 2004). The O⁶-meG /T lesions are efficiently recognized by the MSH2-MSH6 heterodimer (Duckett et al., 1996). Importantly, MGMT is down-regulated in a variety of cancers which may lead to an increase in O⁶-meG lesions (Gerson, 2004). In the laboratory MGMT can be inhibited by O⁶-benzylguanine, which acts as a pseudo-substrate for the repair protein. Much of the work done to elucidate the MMR-dependent response to alkylation damage has been performed using cancer cell lines, and treatment of a MMR-proficient cancer cell line with MNNG results in activation of the DNA damage response including a permanent G₂ cell cycle arrest and apoptosis through activation of ATM/ATR and downstream cell cycle checkpoint kinases Chk1 and Chk2 in a MMR dependent-manner (Hickman and Samson, 2004; Stojic et al., 2004b; Mastrocola and Heinen, 2010a). Interestingly, activation of the G₂ cell cycle arrest requires two rounds of DNA replication (Stojic et al., 2004b).

Two models that are not mutually exclusive have been proposed to account for the role of MMR in this DNA damage response. The "futile cycle" model proposes that O⁶-meG/T mismatches formed during the first round of DNA replication will trigger repeated rounds of MMR-provoked excision and resynthesis due to the inability of the pathway to repair the modified base in the parent strand. This process will generate stretches of single-strand DNA that will be converted into cytotoxic double-strand DNA breaks if left to persist into the second round of DNA replication (Figure 1-2) (Goldmacher et al., 1986; York and Modrich, 2006). Alternatively, the direct signaling model proposes that the MMR machinery directly recruits DNA checkpoint signaling proteins like ATR and Chk1

to the sites of the DNA lesion to initiate and propagate the signal (Figure 1-2) (Lin et al., 2004; Yang et al., 2004). Since the mechanism of the MMR-dependent DNA damage response was mainly studied using transformed cell lines, we wished to further study this damage response in a nontransformed human cell model. Thus, in this study we investigated the MMR-dependent damage response to MNNG in human pluripotent stem cells and human intestinal organoids.

C. Human pluripotent stem cells

Human pluripotent stem cells (hPSCs) include human embryonic stem cells (hESCs) and induced pluripotent stem cells (iPSCs). They are able to differentiate to all three germ layers and give rise to all the different somatic cell lineages. They can replicate indefinitely in culture as nontransformed cells. These features make PSCs a good cell model for us to study the MMR-dependent DNA damage response in normal human cells. hPSCs are also unique in that they have enhanced DNA repair activities to strictly maintain genome stability to protect the developing embryo from the damaging effects of mutations. Many studies have shown that hPSCs are highly efficient at removing DNA damage compared to somatic cells (Adams et al., 2010; Fung and Weinstock, 2011; Luo et al., 2012; Maynard et al., 2008). DNA damage caused by gamma-irradiation, ultra-violet irradiation, H₂O₂ or cross-linking agents are repaired more rapidly in hESCs than in primary human fibroblasts (Maynard et al., 2008). However, hPSCs also have very low tolerance for unrepaired DNA damage and react by a robust damage response leading to apoptosis (Momcilovic et al., 2010; Luo et al., 2012). In Chapter 2 of this study, we examined the activity of the MMR pathway in hPSCs. We particularly

Figure 1-2.

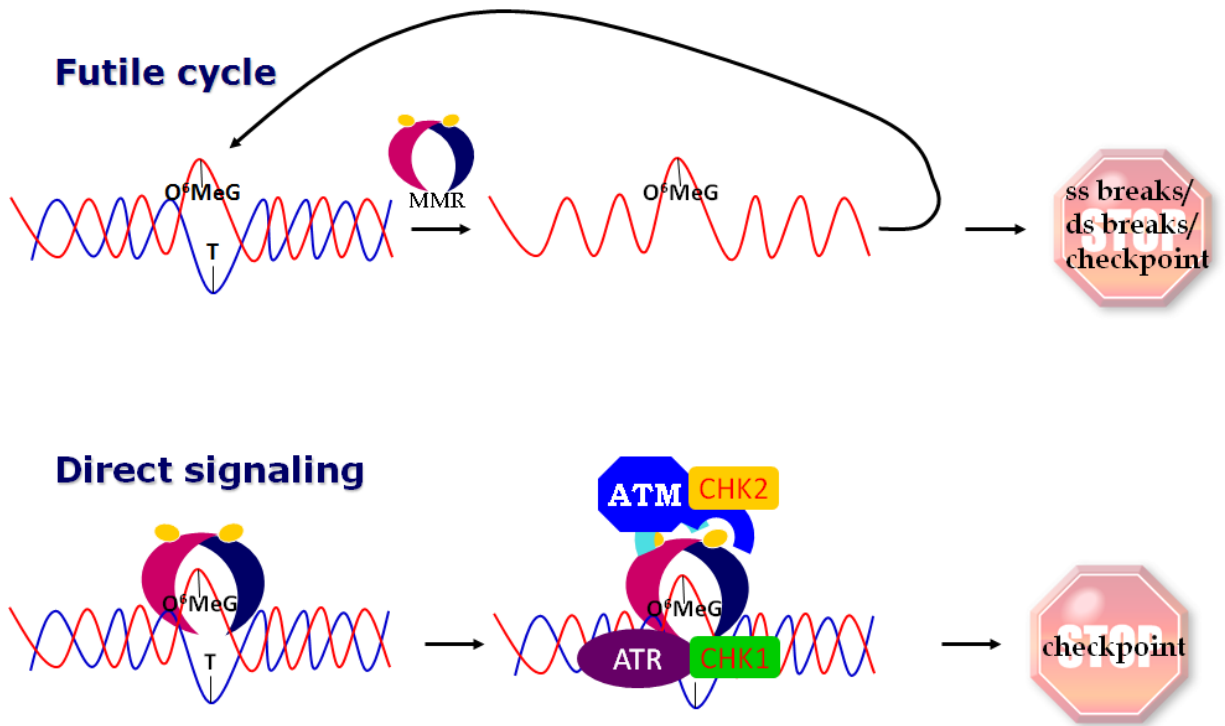


Figure 1-2. Proposed models for activation of the MMR-dependent DNA damage response.

In both models activation of the DNA checkpoint response requires the initial recognition of the DNA lesion (in this case an O⁶-meG/T mismatch). The futile cycle model (upper) suggests that recognition by the MSH2-MSH6 heterodimer triggers downstream MMR events including excision; however, since the lesion is in the template strand, resynthesis will yield an unrepaired lesion. Subsequent rounds of mismatch-provoked excision and resynthesis, the "futile" cycle, will lead to the generation of a double-strand break and the activation of the DNA checkpoint response. In the direct signaling model (lower), DNA associated MSH2-MSH6/MLH1-PMS2 protein complexes act as damage sensors and directly recruit factors involved in the DNA checkpoint activation.

investigated whether hPSCs are capable of eliciting the MMR-dependent damage response to alkylation damage as observed in human cancer cell lines and other somatic cell types.

D. Intestinal organoids

In recent years, a series of protocols have been developed to culture human intestinal cells in three dimensional organoids. Organoids are stem cell-derived human epithelial "mini-organs". Human intestinal organoids (HIOs) have been created from intact intestinal crypts as well as through the directed differentiation of hESCs (Cao et al., 2011; Sato et al., 2011; Spence et al., 2011). Intestinal epithelium consists of millions of crypts and within each crypt there is a hierarchy of different cell types. A typical colonic crypt has the intestinal stem cells (ISCs) (marked by Lgr5) at the bottom of the crypt, which are essential for rapid turnover of the epithelium, transient amplifying (TA) cells which divide rapidly and then differentiate into nondividing mature cell types such as goblet cells, enterocytes, enteroendocrine cells and tuft cells (Figure 1-3) (Barker, 2014). Wnt signaling is essential for maintaining and promoting the proliferation of ISCs which are thought to be the cell of origin of colorectal cancer (White and Lowry, 2015). HIOs have been shown to be self-renewing in culture while displaying markers of differentiated intestinal epithelium when provided with the appropriate growth factors suggesting that they recapitulate the different cell types found in the human intestine. It is especially useful for us to study the MMR-dependent DNA damage response in the tissue of origin and assess whether this response is active in normal human intestinal cells and can play a role in tumor suppression in Lynch syndrome. Thus, in Chapter 3,

Figure 1-3.

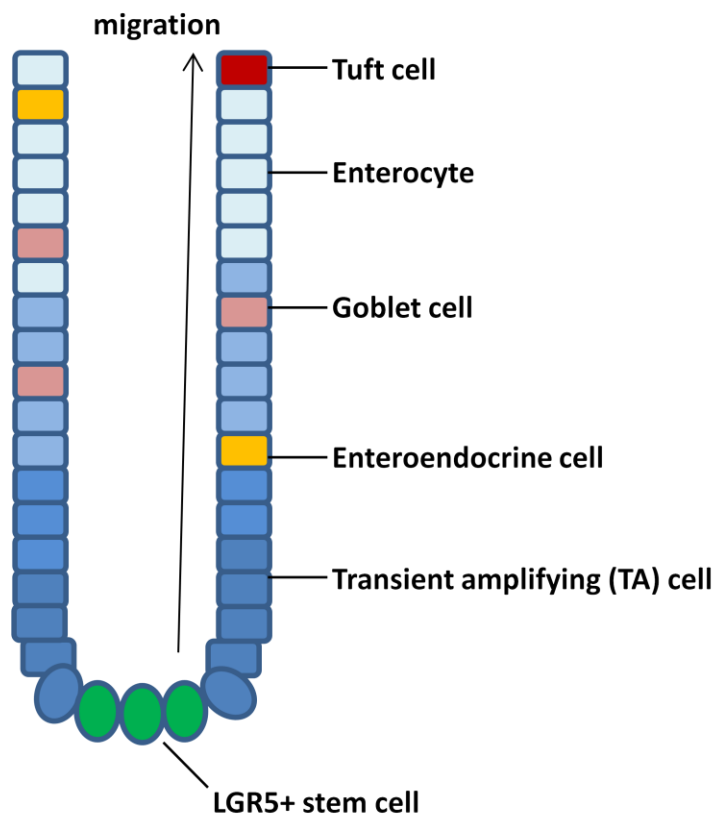


Figure 1-3. Architecture of the colon crypt.

LGR5⁺ stem cells at the crypt base generate rapidly proliferating TA cells in the lower half of the crypt. TA cells subsequently differentiate into the mature lineages of the surface epithelium (goblet cells, enterocytes, enteroendocrine cells and tuft cells). Epithelial turnover occurs every 5–7 days.

we have studied the MMR-dependent DNA damage response to alkylation damage in HIOs to gain some insights into how loss of MMR may contribute to early events of tumorigenesis in Lynch syndrome.

E. Senescence

Cellular senescence is a phenomenon where by proliferating cells permanently cease to divide due to a variety of causes such as telomere dysfunction, oxidative stress, non-telomeric DNA damage, and oncogene activation. One possible consequence that has been linked to senescence is aging, as the number of senescent cells is much higher in old animals comparing to young animals during normal aging (Childs, 2015), and recent evidence has shown that eliminating senescent cells can actually delay age-related dysfunction (Baker, 2011). There is also strong evidence that cellular senescence is a potent anticancer mechanism (Campisi, 2001; Braig, 2006; Prieur, 2008; Guerra, 2011). Thus, senescence is commonly represented as a double-edged sword. Although senescent cells can no longer replicate, they remain metabolically active and commonly adopt an immunogenic phenotype consisting of a pro-inflammatory secretome. This senescence associated secretory phenotype (SASP) consisting of inflammatory cytokines, growth factors, and proteases is a highly characteristic feature of senescent cells (Campisi, 2007). The SASP can have positive or negative effects on cancer depending on the context. The SASP cytokines can reinforce the senescence growth arrest and induce senescence in neighboring cells in a paracrine fashion. The pro-inflammatory factors can also recruit immune cells to the local site and promote immune clearance of the damaged cells (Xue, 2007; Chung, 2009). All of these are

beneficial in defense against cancer. On the other hand, these cytokines can also cause epithelial-to-mesenchymal transitions which promote cancer (Sparmann, 2004; Tamm, 1994). In this study, we have examined whether the MNNG treatment induced senescence in HIOs as a MMR-dependent DNA damage response to alkylation damage in intestinal cells and the possible implication in tumorigenesis in Lynch syndrome.

CHAPTER 2

Human Pluripotent Stem Cells Have a Novel Mismatch Repair-Dependent Damage Response

Lin B., Gupta D., Heinen C.D. (2014). J Biol Chem. 29;289(35):24314-24.

A. ABSTRACT

Human pluripotent stem cells (PSCs) are presumed to have robust DNA repair pathways to ensure genome stability. PSCs likely need to protect against mutations that would otherwise be propagated throughout all tissues of the developing embryo. How these cells respond to genotoxic stress has only recently begun to be investigated. Although PSCs appear to respond to certain forms of damage more efficiently than somatic cells, some DNA damage response pathways such as the replication stress response may be lacking. Not all DNA repair pathways, including the DNA mismatch repair (MMR) pathway, have been well characterized in PSCs to

date. MMR maintains genomic stability by repairing DNA polymerase errors. MMR is also involved in the induction of cell cycle arrest and apoptosis in response to certain exogenous DNA-damaging agents. Here, we examined MMR function in PSCs. We have demonstrated that PSCs contain a robust MMR pathway and are highly sensitive to DNA alkylation damage in an MMR-dependent manner. Interestingly, the nature of this alkylation response differs from that previously reported in somatic cell types. In somatic cells, a permanent G2/M cell cycle arrest is induced in the second cell cycle after DNA damage. The PSCs, however, directly undergo apoptosis in the first cell cycle. This response reveals that PSCs rely on apoptotic cell death as an important defense to avoid mutation accumulation. Our results also suggest an alternative molecular mechanism by which the MMR pathway can induce a response to DNA damage that may have implications for tumorigenesis.

B. INTRODUCTION

Human pluripotent stem cells (PSC), including embryonic stem cells (ESC) and induced pluripotent stem cells (iPSC) can replicate indefinitely in culture and give rise to all the different somatic cell lineages. These features make PSCs attractive for their potential use in regenerative therapy, and as a useful model system for drug screening, genotoxicity testing and general mechanistic studies of development. The role of these cells in the early stages of human development likely requires a strict maintenance of genome stability to protect the developing embryo from the damaging effects of mutations. Not surprisingly, some of the initial studies examining DNA repair pathways

in PSCs indicate they are highly efficient at removing DNA damage compared to somatic cells (Adams, 2010; Fung, 2011; Luo, 2012; Maynard, 2008). DNA damage caused by gamma-irradiation (IR), ultra-violet irradiation (UV), H₂O₂ or the crosslinking reagent psoralen are repaired more rapidly in hESC lines than in primary human fibroblasts (Maynard, 2008).

However, in addition to damage repair, cells can respond to genotoxic stress through the induction of protective cell cycle checkpoints. As an example, impeded replication forks result in activation of an S-phase checkpoint which leads to stabilization of the replication fork and coordination of DNA repair with the resumption of DNA synthesis (Branzei, 2009). This important damage response protects the viability of the cell while at the same time reduces the incidence of broken chromosomes which can lead to genomic rearrangements. Interestingly, PSCs have been reported to lack this S-phase checkpoint in response to replication stress (Desmarais, 2012). Rather PSCs upon encountering replication stress are much more prone to apoptosis. This same increased propensity to undergo apoptosis is also observed in PSCs treated with UV and IR (Luo, 2012; Qin, 2007; Wilson, 2010; Momcilovic, 2010; Fillion, 2009). Understanding the response of PSCs to different sources of genotoxic stress and the molecular mechanisms involved becomes crucial if these cells are to ever realize their potential for therapeutic purposes.

An important repair pathway that needs to be examined in PSCs is the DNA mismatch repair (MMR) pathway. MMR increases the fidelity of DNA replication by up to three orders of magnitude to maintain genome integrity through correcting DNA polymerase

errors that escape proofreading (Kunkel, 2005; Kolodner, 1999; Modrich, 2006). Loss of MMR function has been proposed to create a mutator phenotype in cells that increases the risk of tumorigenesis (Fishel, 1995). Consistent with this hypothesis, germline mutations in the major MMR genes are associated with the inherited cancer predisposition disease Lynch syndrome (Lynch, 2009). Defects in MMR, mostly due to epigenetic inactivation of the MMR gene MLH1, have also been associated with 10-40% of sporadic colorectal and other cancer types (Dietmaier, 1997; Kane, 1997). In addition to repairing DNA polymerase mistakes, the MMR pathway is also required for activation of cell cycle checkpoints and apoptosis in response to certain DNA damaging agents (Stojic, 2004a). For example, MMR-deficient cells are up to 100-fold more resistant to the SN-1 alkylating agent N-methyl-N'-nitro-N-nitrosoguanidine (MNNG) than isogenic MMR-proficient cells (Cejka, 2003a; Kaina, 1997; Mastrocola and Heinen, 2010a). Studies in multiple cell lines have revealed that treatment with MNNG induces a MMR-dependent G₂ arrest in the second cell cycle after treatment (Kaina, 1997; Cejka, 2003b; Mastrocola and Heinen, 2010b). It is not clear why it takes two cell cycles to induce the G₂ arrest. The primary cytotoxic lesion generated by MNNG is O⁶-methylguanine (MeG), which is commonly mispaired with T during replication. The MeG-T mispair is recognized by the MMR heterodimer MSH2-MSH6 which activates the MMR response (Duckett, 1996). Two major models have been proposed to explain the molecular mechanism of this damage response. The "futile cycle" model suggests that the MeG-T mispair generated during the first S-phase after treatment with MNNG initiates the MMR process. Successful MMR is executed leading to excision of the mispaired T in the daughter strand. However, as the modified MeG remains in the

template strand, the polymerase will regenerate a MeG–T mispair again during repair synthesis. The MMR process will be triggered repeatedly resulting in an unrepaired gap opposite the lesion. In the next S-phase, the new replication fork encounters this gap and converts it to a double strand break. It is this double strand break which initiates a DNA damage response that ultimately leads to cell cycle arrest and eventual apoptosis. The second model, the “direct signaling” model, suggests that, following binding of the MeG-T mismatches by the MMR proteins a damage signal is transmitted directly to the checkpoint machinery without the need for DNA processing. Evidence supporting the direct signaling model includes findings that overexpression of MSH2 or MLH1 induces apoptosis in either MMR proficient or deficient cells (Zhang, 1999), and that checkpoint kinases Chk1, Chk2, ATR and ATM co-immunoprecipitate with MSH2 in cell extracts after MNNG treatment (Adamson, 2005; Liu, 2010; Wang, 2003; Yoshioka, 2006).

In this study, we examined the activity of the DNA MMR pathway in human PSCs. We were particularly interested in determining whether PSCs are capable of eliciting the MMR dependent damage response to alkylation damage as observed in human cancer cell lines and other somatic cell types. Our results reveal that iPSCs and ESCs are hypersensitive to the alkylating agent MNNG, although the mechanism by which they respond to the DNA damage is different. Our results demonstrate that the MMR pathway is an important repair pathway for maintaining genome stability in human PSCs. These results also reveal the need for further studies to fully understand the mechanisms by which the MMR pathway can elicit a DNA damage response.

C. MATERIALS AND METHODS

Cell Culture

Human ESCs (H1, CT-2) were obtained from the University of Connecticut Stem Cell Core. Human iPSCs YK26 were reprogrammed from human dermal fibroblasts (HDFa) using retroviral vectors as described (Zeng, 2010) and Rx13 were reprogrammed from BJ human foreskin fibroblasts (HFF) using a single excisable polycistronic lentiviral Stem Cell Cassette (STEMCCA) encoding the Yamanaka factors at the University of Connecticut Stem Cell Core facility. Both ESCs and iPSCs were cultured on BD Matrigel (BD Biosciences) with irradiated mouse embryonic fibroblast-conditioned ESC media (GlobalStem) containing DMEM-F12, 20% knockout serum replacer (Invitrogen), non-essential amino acids (NEAA, Invitrogen), 1mM L-glutamine (Invitrogen), 0.1mM beta-mercaptoethanol (Sigma) and 4 ng/ml basic Fibroblast Growth Factor (bFGF, Invitrogen). HDFa cells (ATCC) and human foreskin fibroblasts (HFF) (ATCC) were cultured in DMEM containing 10% fetal bovine serum (FBS, Gibco), and NEAA. Hec59 cells (kind gift of Drs. Thomas Kunkel and Alan Clark) were grown in DMEM/F12 containing 10% FBS. HeLa cells (ATCC) were grown in DMEM containing 10% FBS.

Western Blotting

An equal number of H1, CT-2, YK26, Rx13, HDFa, HFF, HeLa or Hec59 cells were harvested and lysed with RIPA buffer supplemented with protease inhibitors. The cell lysates were separated by electrophoresis on a 6% SDS-polyacrylamide gel. The primary antibodies used included: anti-MSH2 (BD #556349), anti-MSH6 (Bethyl A300-

023A), anti-MLH1 (BD #550838), anti-PMS2 (BD #556415), anti-PCNA (Santa Cruz sc-56), anti-pol δ (Santa Cruz sc-10784), anti-RFC4 (Santa Cruz sc-20996), antiRPA (Calbiochem RPA34-20), anti-phospho-Chk1 (Ser 345) (Cell Signaling #2341), anti-phosphoChk2 (Thr 68) (Cell Signaling #2661), anti-Chk1 (Cell Signaling #2345), anti-Chk2 (Cell Signaling #2662), anti- γ H2AX (Ser 139) (Millipore 05-636), anti-phospho-p53 (Ser15) (Cell Signaling #9284), anti-p53 (Cell Signaling #9282), anti-phospho-ATM (Ser 1981) (cell signaling #5883), anti-phospho-ATR (Ser 428) (cell signaling #2853), anti-ATM (cell signaling #2873), anti-ATR (cell signaling #2790) and anti-actin (Sigma A5060). Where indicated, cells were treated with 10 μ M of the ATM-specific inhibitor KU5593 (Selleck Chemicals) and/or the ATR-specific inhibitor VE-821 (Selleck Chemicals) for 24 hours prior to harvesting.

MNNG Treatment and Cell Cycle Analysis

MNNG (obtained from the National Cancer Institute Chemical Carcinogen Reference Standard Repository; CAS: 70-25-7) was dissolved in DMSO to a concentration of 10 mM and stored at -20°C until use. O⁶-Benzylguanine (O⁶-BG; CAS: 19916-73-5) was purchased from Sigma, dissolved in DMSO to a concentration of 25 mM and stored at -80°C until use. Cells were treated with 25 μ M O⁶-BG for 2 hours, then media was replaced with fresh media containing 25 μ M O⁶-BG and 2 μ M MNNG for 48 hours. Cell cycle analyses were performed using propidium iodide (PI) staining for DNA content and subsequent detection by flow cytometry. Briefly, cells were harvested and fixed in 70% ethanol at -20°C . Cells were then treated with 20 $\mu\text{g/mL}$ PI and 200 $\mu\text{g/mL}$ RNase A and incubated at 37°C for 1 hour, filtered, and analyzed with a FACS Calibur flow

cytometer (BD Biosciences). The resulting data were analyzed by Modfit analysis software.

MMR Knockdown

MMR knockdown YK26 cells were generated with lentiviral vectors containing shRNAs targeting either MSH2 or MLH1. shMSH2 and sh-MLH1 lentiviruses were a kind gift from Drs. Kareem Mohni and Sandra Weller. Briefly, YK26 cells were incubated with lentivirus containing sh-MSH2 or sh-MLH1 for 1 hour, and then fresh medium was added to continue incubation overnight. Stable expression of the shRNAs was maintained by adding 0.8 µg/ml puromycin to the normal media.

Annexin V Staining and Apoptosis Analysis

YK26 cells were treated with 2 µM MNNG for 24 hours and then harvested and stained with anti-Annexin V and PI using the Annexin V apoptosis kit (Molecular Probes v13241). The cells were analyzed with a LSRII flow cytometer (BD Biosciences). The resulting data were analyzed by FlowJo analysis software.

Cell Synchronization

Synchronization in mitosis was performed by treating YK26 cells with 0.2 µM nocodazole for 18 hours. Cells were released in fresh medium containing 25 µM O6 - BG. At four hours post release, cells were treated with 2 µM MNNG for an additional 4

hours. Cells were harvested at different time points as indicated and subjected to cell cycle analysis.

MMR Assay

The heteroduplex MMR substrate was prepared according to Zhou et al., (Zhou, 2009). The p111 and p189 plasmids were a kind gift from Dr. LuZhe Sun. p189 encodes for a premature stop codon in the EGFP gene. To generate single-stranded (ss) DNA circles, p111 was nicked with Nb.Bpu10I (Thermo Scientific) and further digested with ExoIII (New England Biolabs). The heteroduplex substrate was prepared by annealing the ssDNA circles to linearized, denatured p189 DNA. Excess linear DNA and ssDNA were removed by plasmid-safe DNase (Epicentre Biotechnologies). To assess MMR activity, PSCs were transfected with 2.5 µg of the heteroduplex plasmid and 2.5 µg of pDsRed2-N1 (Clontech) which encodes the red fluorescent protein (RFP) using the Amaxa Human Stem Cell Nucleofector kit 2 (Lonza VPH- 5022). HeLa cells were transfected using Lipofectamine2000 (Invitrogen) and HDFa cells were transfected using GeneIn transfection reagent (GlobalStem). After incubation for 48 hours the cells were harvested and analyzed for fluorescence intensity with a LSRII flow cytometer (BD Biosciences) using BD FACS Diva software. The ratio of GFP-positive cells to RFP-positive cells was determined to account for differences in transfection efficiency.

Immunofluorescent staining

H1 cells with or without MNNG treatment were fixed with 4% paraformaldehyde for 10 minutes, and permeablized with cold acetone for 2 minutes. After blocking in 1%BSA/PBS for 1 hour at room temperature, cells were incubated with the diluted primary antibodies anti-cleaved caspase-3 (BD #559565) and anti-cleaved caspase-9 (Pierce #PA5-17913) for 1 hour at room temperature then incubated with diluted Alexa Fluor 488 secondary antibody (Molecular Probes) for 45 minutes at room temperature. Nuclei were counterstained with 4',6-diamidino-2-phenylindole (DAPI) and cells were analyzed on a Nikon Eclipse Inverted Fluorescent microscope.

D. RESULTS

The MMR proteins are highly expressed in PSCs compared to parental fibroblasts

To begin characterizing the MMR pathway in iPSCs, we first examined the expression of the four major MMR proteins, MSH2, MSH6, MLH1 and PMS2. Whole cell extracts were prepared from an equal number of human dermal fibroblasts (HDFa), human foreskin fibroblasts (HFF), human ESCs (H1, CT-2) and human iPSCs (YK26 reprogrammed from HDFa, Rx13 reprogrammed from BJ foreskin fibroblasts). Consistent with previous reports of increased MMR gene expression in iPSCs (Momcilovic, 2010), we showed that the expression of all four MMR proteins are increased 5-8 fold in YK26 cells compared to the parental HDFa cells (Fig.2-1A) and similarly increased in H1 and Rx13 cells compared to HFF cells (Fig.2-1B). The

Figure 2-1.

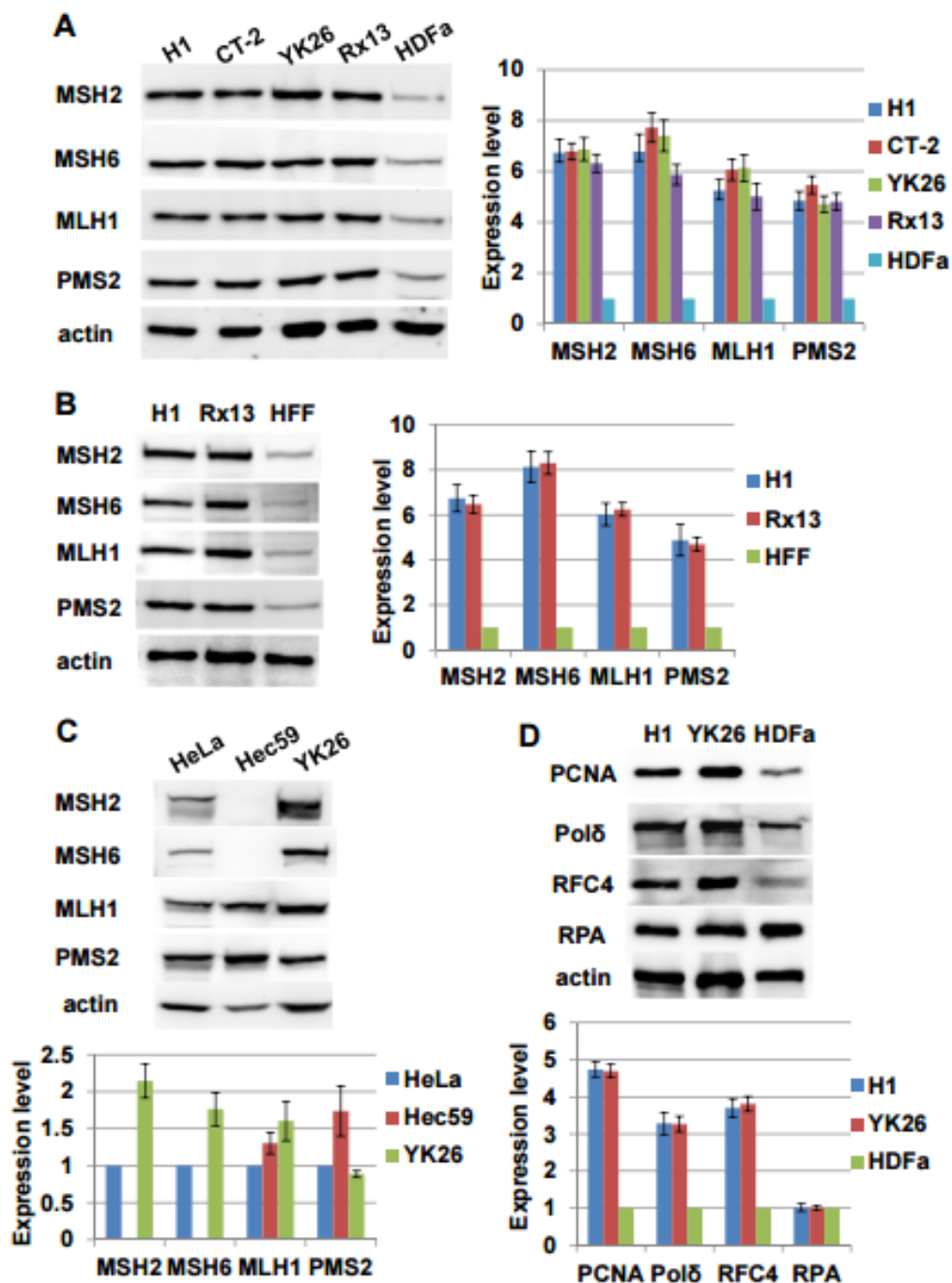


Figure 2-1. Human pluripotent stem cells express higher levels of MMR proteins than parental fibroblasts.

A, Western blot analysis of mismatch repair (MMR) proteins in an equal number of human embryonic stem cells (H1, CT-2), human induced pluripotent stem cells (YK26, Rx13) and parental fibroblasts (HDFa). B, Western blot analysis of MMR proteins in an equal number of H1, Rx13 and human foreskin fibroblasts (HFF).C, Western blot analysis and quantitation of MMR proteins in HeLa, Hec59 and YK26 cells.D, Western blot analysis of various replication proteins in H1, YK26, and HDFa cells. The values represent the means of three independent experiments.

expression between the different iPSCs and ESCs was similar (Fig. 2-1A and 2-1B). PSCs undergo rapid cell division compared to both fibroblast lines, so we compared expression of the MMR proteins in the PSC lines to a more proliferative cell type. We found that the levels of MSH2, MSH6 and MLH1 in YK26 cells were 1.5-2 fold higher than in the MMR-proficient HeLa cervical cancer cells, while PMS2 levels were similar (Fig. 2-1C). These results suggest that PSCs may have a robust MMR system to protect their genome. We also found that essential replication proteins such as PCNA, Pol δ , and RFC4 were expressed at higher levels in PSCs compared to fibroblasts, though levels of RPA were similar between the cell types (Fig. 2-1D).

PSCs repair mismatches more efficiently than parental fibroblasts

Considering the increased expression of MMR proteins in PSCs, we asked whether their single basepair mismatch repair capacity is enhanced compared to the parental fibroblasts. To test repair activity, we introduced a plasmid into cells that encodes GFP containing a single G-T mispair that disrupts protein translation (Zhou, 2009). In vivo repair of the mismatch leads to restored GFP expression that can be quantitated using flow cytometry. As a control for transfection efficiency, cells were co-transfected with an RFP-expressing plasmid. We found that the majority of transfected ESCs and iPSCs expressed GFP indicating robust repair of the heteroduplex substrate (Fig. 2-2A and 2-2B). This repair efficiency was significantly enhanced over parental HDFa cells. The repair rate in PSCs was similar to MMR-competent HeLa cells (Fig. 2-2A and 2-2B). To confirm that restoration of GFP expression is MMR dependent, we used lentiviral

Figure 2-2.

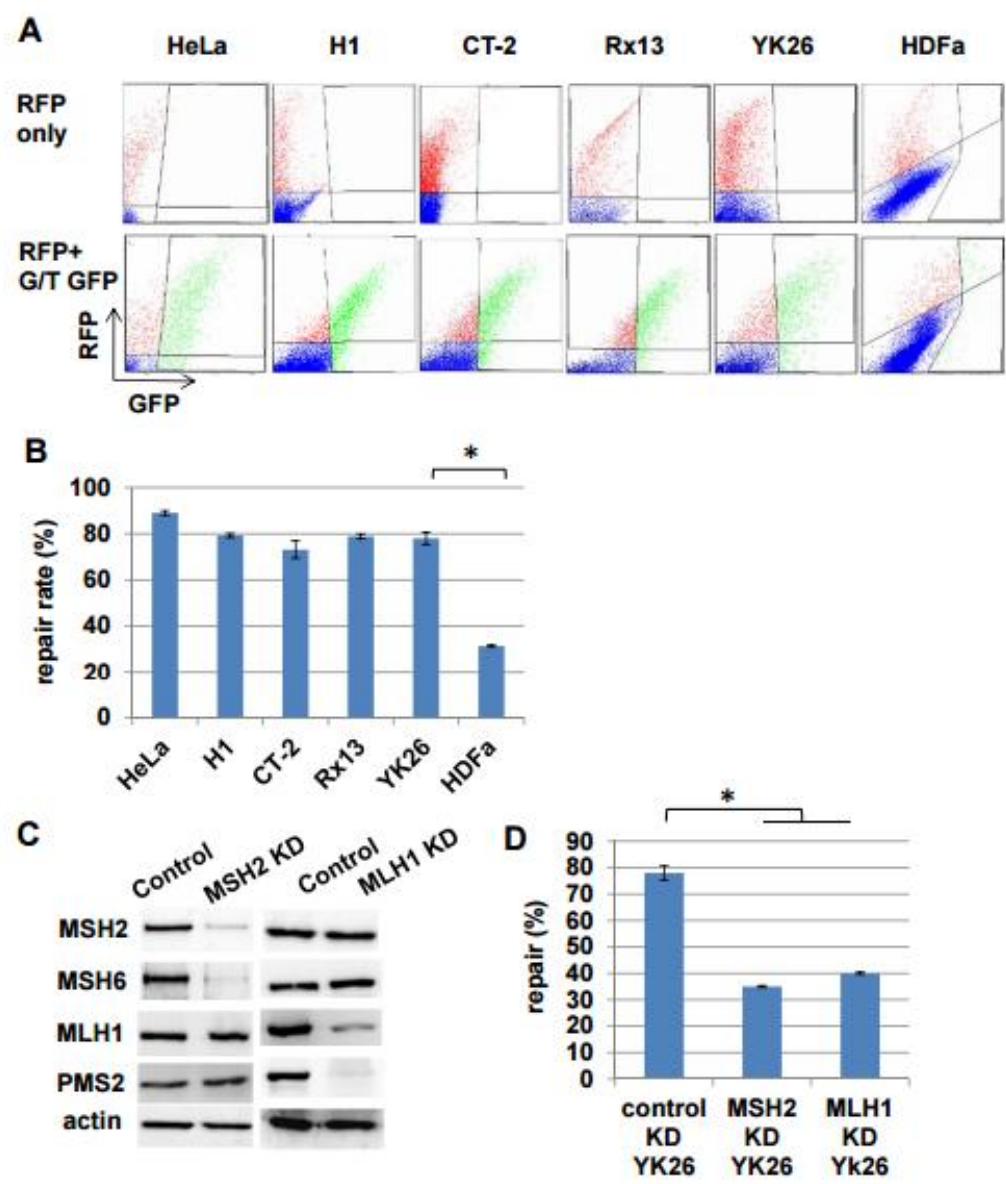


Figure 2-2. Human pluripotent stem cells repair mismatches more efficiently than parental fibroblasts.

Repair of a transfected heteroduplex plasmid encoding GFP with a premature stop codon and RFP as a transfection control as measured in HeLa, H1, CT-2, YK26, Rx13 and HDFa cells. A, Representative flow cytometry images. B, Quantitation of repair rates in transfected cells. * represents pvalue < 0.01. C, Western blot analysis confirming the knockdown of MSH2 or MLH1 in YK26. Actin is included as a loading control. D, The percentage of heteroduplex repair in control and MSH2 or MLH1 knockdown (KD) YK26 cells. The values represent the means of three independent experiments. * represents p-value < 0.01.

vectors encoding shRNAs to knockdown levels of MSH2 or MLH1 in the YK26 cells (Fig. 2-2C). Knockdown of MSH2 or MLH1 also resulted in loss of stability of their obligate heterodimer partners MSH6 and PMS2, respectively. Knockdown of MSH2 did not affect levels of MLH1-PMS2, nor did MLH1 knockdown alter levels of MSH2-MSH6 (Fig. 2-2C). We found that the levels of repair in either MSH2 knockdown or MLH1 knockdown YK26 cells was 2-2.5 fold reduced compared to YK26 cells infected with a luciferase shRNA expressing lentivirus (Fig. 2-2D). These results reveal that PSCs have robust MMR repair function compared to differentiated cell types that is similar to that observed in highly proliferative cancer cells.

PSCs are hypersensitive to the alkylating agent MNNG

To test whether PSCs have the protective MMR-dependent response to alkylation damage, we treated ESCs and iPSCs, along with HeLa cells (MMR proficient), Hec59 endometrial cancer cells (MMR deficient, see Fig. 2-1C), and HDFa cells with 2 μ M MNNG for 48 hours. Cells were pretreated with the methylguanine methyltransferase inhibitor O6-BG for 2 hours to enhance the effects of the alkylation damage. The cells were examined by flow cytometry to determine whether MNNG induces a cell cycle arrest. Consistent with our previous studies (Mastrocola and Heinen, 2010a; 2010b), HeLa cells were permanently arrested at G2/M after MNNG treatment, while no cell cycle arrest was observed in the MMR-deficient Hec59 cells (Fig. 2-3A). Surprisingly, while we did not see any evidence for a G2/M arrest in either the iPSC or ESC lines, we observed large sub-G1 peaks consistent with the cells undergoing apoptosis (Fig. 2-3A

Figure 2-3.

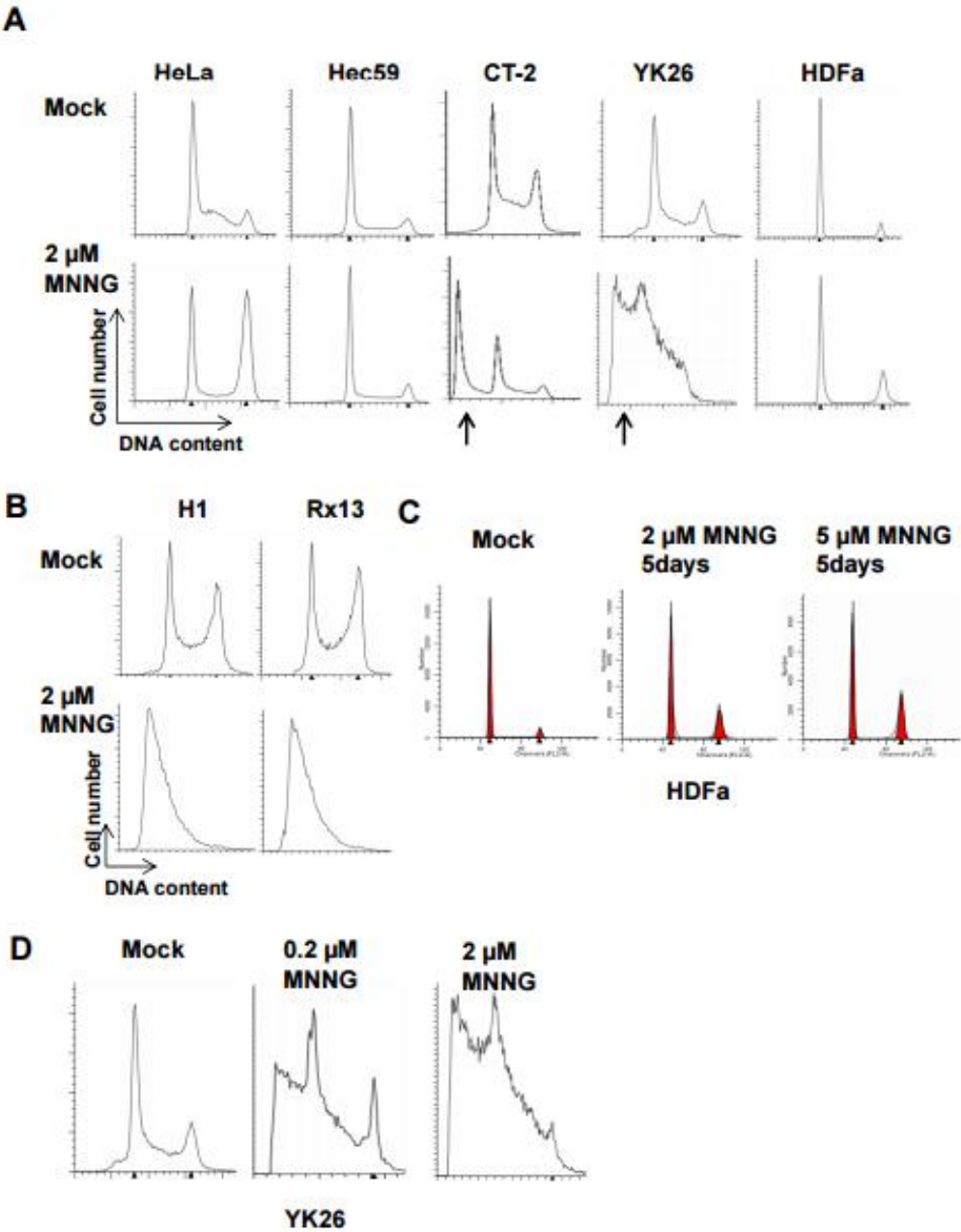


Figure 2-3. DNA alkylation damage induces apoptosis in human pluripotent stem cells.

A, Representative cell cycle profiles of HeLa, Hec59, CT-2, YK26, and HDFa cell lines with or without 2 μ M N-methyl-N'-nitro-N-nitrosoguanidine (MNNG) for 48 hours as measured by flow cytometry. The arrows indicate the presence of sub-G1 populations, associated with apoptotic cells. B, Representative cell cycle profiles of H1 and Rx13 cells with or without 2 μ M MNNG for 48 hours. C, Representative cell cycle profiles of HDFa cells with or without 2 μ M or 5 μ M MNNG for 5 days. D, Representative cell cycle profiles of YK26 cells mock treated or treated with 2 μ M or 0.2 μ M MNNG.

and 2-3B). The fibroblasts from which the YK26 iPSCs were derived did not show any apoptosis and only a modest G2/M arrest after MNNG treatment. As the HDFa cells replicate more slowly than PSCs and HeLa cells, we incubated them for an additional 72 hours following treatment to ensure that the cells could finish the two cell cycles necessary to undergo a G2/M arrest consistent with the futile cycle model. We also tested a higher dose of MNNG. These changes led to slightly increased populations of cells in G2/M, but still not the dramatic response observed in HeLa cells suggesting that the MMR-dependent response to alkylation damage is not very strong in HDFa cells (Fig. 2-3C). On the other hand, treatment of iPSCs with a ten-fold lower concentration of MNNG for 48 hours still resulted in a substantial sub-G1 population (Fig. 2-3D). These results highlight the extent to which the iPSCs re-activate the alkylation damage response during reprogramming.

The alkylation damage response is MMR dependent

We next tested whether the response to MNNG in PSCs is MMR dependent by comparing the damage response between control and MMR knockdown iPSCs. We treated the control and MMR knockdown iPSCs with 2 μ M MNNG and analyzed their cell cycle profiles. The MNNG induced apoptotic response was entirely abrogated in the MSH2 or MLH1 knockdown lines suggesting that the hypersensitive response of PSCs to alkylation damage is MMR dependent (Fig. 2-4A). To confirm that the sub-G1 populations observed in the cell cycle profiles are apoptotic PSCs, we used an apoptotic marker Annexin V to detect apoptotic cells. We found that after MNNG treatment most

Figure 2-4.

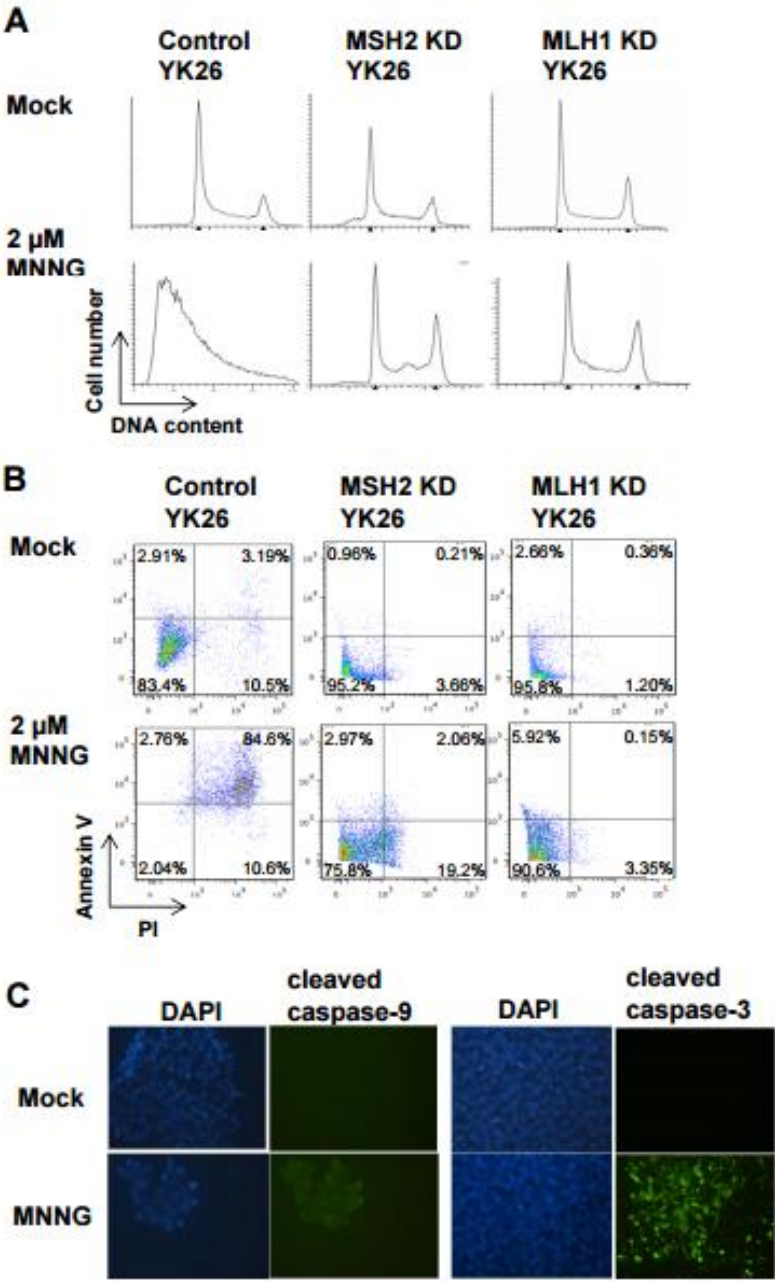


Figure 2-4. The apoptotic response to alkylation damage in induced pluripotent stem cells is mismatch repair dependent.

A, Representative cell cycle profiles of control, MSH2 or MLH1 knockdown YK26 cells with or without 2 μ M MNNG for 48 hours by flow cytometry. B, Annexin V and propidium iodide (PI) staining of control, MSH2 or MLH1 knockdown YK26 cells with or without 2 μ M MNNG treatment for 24 hours as analyzed by flow cytometry. C, Immunofluorescence imaging of cleaved caspase-9 and cleaved caspase-3 in H1 cells with or without 2 μ M MNNG treatment for 24 hours.

of the control YK26 cells were dually-positive for Annexin V and PI, while a majority of the MSH2 or MLH1 knockdown YK26 cells were negative for Annexin V and PI staining (Fig. 2-4B). We also observed activation of caspase-9 and caspase-3 in MNNG-treated YK26 cells by immunofluorescence (Fig. 2-4C). These results demonstrate that PSCs respond to MNNG by inducing an intrinsic apoptotic pathway that is MMR dependent.

MNNG-induced apoptosis occurs in the first S phase after damage without undergoing G2 arrest

Previous studies have shown that MNNG induces a MMR-dependent G2/M arrest in the second cell cycle after treatment in multiple somatic cell types, and this permanent G2/M arrest eventually leads to apoptosis (Kaina, 1997; Cejka, 2003b; Mastrocola and Heinen, 2010b). In both the ESCs and iPSCs, we observed apoptosis after MNNG treatment without any apparent G2/M arrest. We speculated that due to the rapid proliferation rate of PSCs, it was possible the cells underwent a G2/M arrest prior to apoptosing that we failed to observe due to the timing of our experiment. To assess the timing of the response, we synchronized YK26 cells in mitosis with the microtubule inhibitor nocodazole. The cells were then released back into the cell cycle in normal growth media. At 4h post release when most cells were in G1 phase, we treated them with 2 μ M MNNG for an additional 4 hours. We returned the cells to normal media again and harvested them at different time points for cell cycle profile analysis (Fig. 2-5). We observed that our mock treated cells were beginning to enter S-phase 8 hours after release from the nocodazole block and by 16 hours they had all cycled through to G2/M.

Figure 2-5.

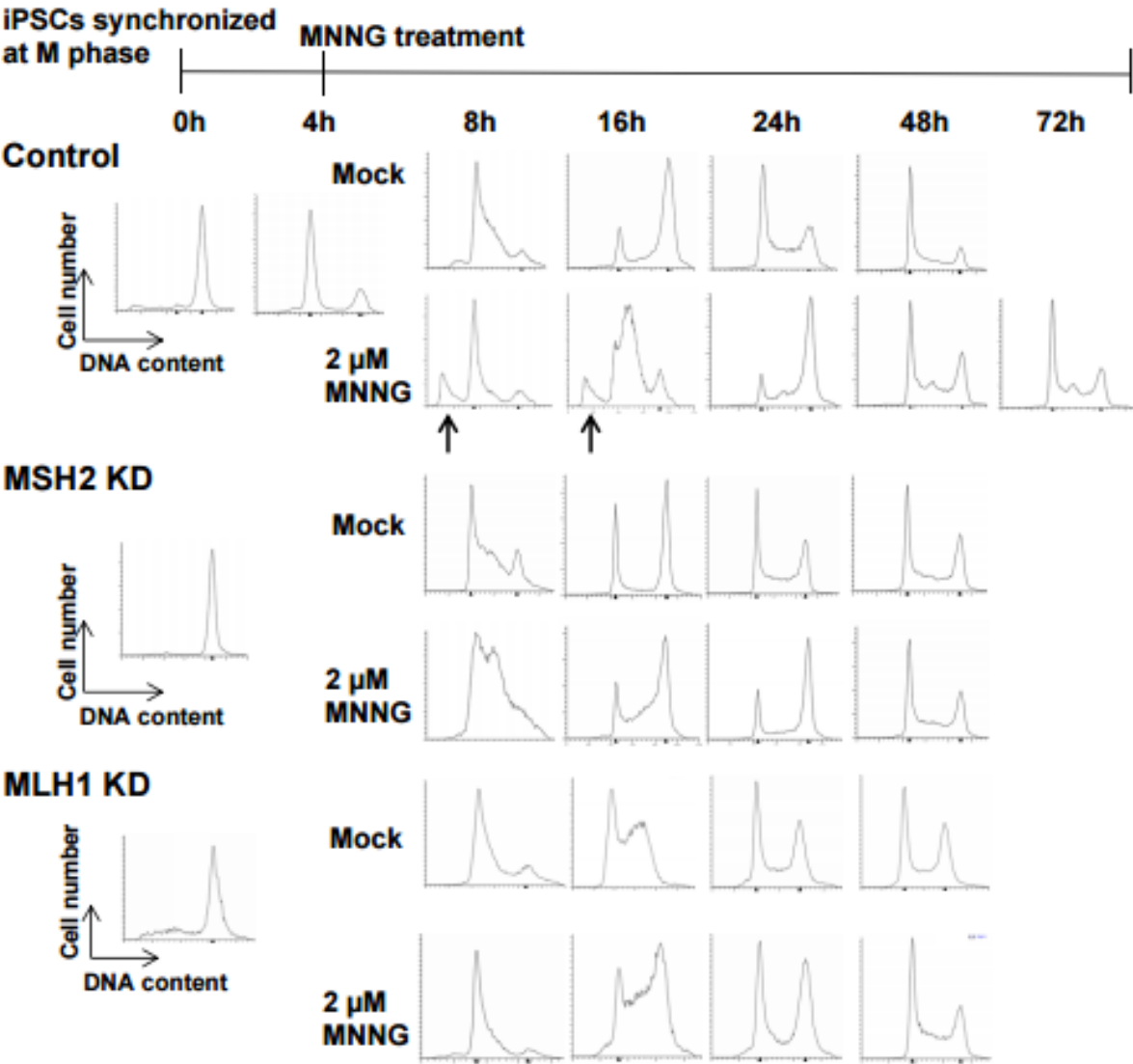


Figure 2-5. MNNG-induced apoptosis occurs in a mismatch repair-dependent manner in the first S-phase after damage.

Representative cell cycle profiles of control or MSH2 knockdown YK26 cells originally synchronized in mitosis by nocodazole as measured by flow cytometry. Cells were released into normal growth media and then, with or without a 4 hour treatment of 2 μ M MNNG, harvested at different time points after release. The arrows indicate sub-G1 populations of cells. The absence of subG1 populations observed in MSH2 knockdown cells indicates a loss of the apoptotic response observed in control cells.

By 24 hours post-release, the cells were continuing through the cell cycle in an asynchronous fashion. Similarly, our MNNG treated cells were also entering S-phase at the 8 hour time point; however, we observed a fraction of the cells in a sub-G1 population. By 16 hours, the treated cells remained mostly in S-phase suggesting a delay in progression through S-phase compared to the untreated cells. A sub-G1 peak was also evident at 16 hours. By 24 hours, the sub-G1 peak had diminished and the surviving cells continued through the cell cycle. To determine whether the cells incur a G2/M arrest after the second cell cycle following MNNG treatment, we harvested treated cells at 48 and 72 hours post-release, but did not observe any cell cycle arrest. We confirmed that the observed apoptotic response to MNNG was MMR-dependent by repeating the synchronization experiments in our MMR knockdown YK26 cells. As observed in our asynchronous populations, the sub-G1 peak following MNNG treatment is absent in the MSH2 and MLH1 knockdown iPSCs (Fig. 2-5).

Unlike the 48 hour MNNG treatment of PSCs which resulted in nearly 85% of the cells apoptosing (Fig. 2-4B), a 4 hour treatment resulted in the death of only a fraction of the cells. To test whether we had selected for a population of cells that can tolerate this treatment level, we allowed the surviving cells to recover in normal growth media for 24 hours before subjecting them to a second round of MNNG treatment for 4 hours. If the initial treatment led to a selection of resistant cells, we would not expect any response to the second round of MNNG. However, we once again observed that a similar fraction of cells displayed a sub-G1 peak, indicative of apoptosis (Fig. 2-6). Taken together, these results suggest that PSCs undergo an immediate apoptotic response to MNNG in

Figure 2-6.

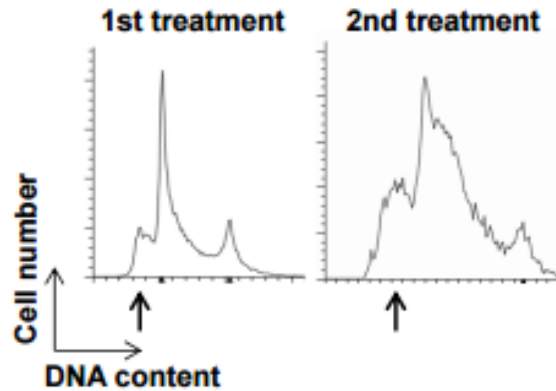


Figure 2-6. Pluripotent stem cells that survive MNNG treatment retain sensitivity to MNNG.

Synchronized YK26 cells were treated with 2 μ M MNNG for 4 hours (1st treatment). Cells were allowed to recover in fresh media for 24 hours, then treated again with 2 μ M MNNG for 4 hours (2nd treatment). Cell cycle profiles of synchronized YK26 after 1st and 2nd treatment are displayed.

the first S-phase after treatment without undergoing a G2/M arrest first. This result is very different from the response observed in HeLa and other somatic cell types.

DNA damage checkpoint kinases are not activated in iPSCs in response to MNNG

Previous studies of the MMR damage response indicate activation of the checkpoint kinases Chk1 and Chk2 following MNNG treatment that may be responsible for the cell cycle arrest and cell death observed (Mastrocola and Heinen, 2010b; Noonan, 2012; Stojic, 2004b). We wanted to test whether the checkpoint kinases are activated in PSCs after MNNG treatment. Asynchronous iPSCs or HeLa cells were mock treated or treated with MNNG for 24 hours and then harvested one day later. We found that HeLa cells treated with MNNG resulted in robust activation of Chk1 and Chk2 as indicated by phosphorylation of Ser 345 and Thr 68, respectively (Fig. 2-7A). No activation of either Chk1 or Chk2 was observed in iPSCs after MNNG treatment (Fig. 2-7A). To confirm that this response was consistent across multiple PSC lines, we performed similar experiments in Rx13 iPSCs and the two ESC lines. As in YK26 cells, MNNG treatment failed to activate Chk1 and Chk2 in this panel of PSCs (Fig. 2-7B). To rule out a transient activation of Chk1 or Chk2 early in the response to damage, we repeated the synchronization experiments described previously and analyzed cell extracts at different time points. We found no significant activation of Chk1 and Chk2 at any point during the cell cycle following MNNG treatment (Fig. 2-7C and 2-7D). However, we did observe a strong induction of γ H2AX which is indicative of double strand breaks and/or replicative stress in the first S phase coinciding with the sub-G1 peaks (Fig. 2-7C and 2-7D). These

results indicate that the typical checkpoint kinases activated during the MMR-dependent damage response in somatic cells are not involved in the PSCs response to alkylation damage, again suggesting a different damage response mechanism is employed in these cells.

p53 is induced and activated in iPSCs after MNNG treatment

PSCs treated with the DNA damaging agent etoposide, undergo a rapid and extensive induction of apoptosis that is abrogated by knocking down p53 (Grandela, 2007). To test whether p53 is activated in PSCs after MNNG treatment, we examined MNNG treated iPSC lysates for increased levels of total p53 protein and increased phospho-p53 (Ser 15) levels. We found that both p53 and phospho-p53 levels were increased in iPSCs after a 24 hour MNNG treatment, however, there was no induction or activation of p53 in MSH2 knockdown YK26 cells (Fig. 2-7E and 2-7F). We observed a similar MNNG-induced activation of p53 in the other iPSC and ESC lines tested (Fig. 2-7B). These results indicate that MNNG treatment causes a MMR-dependent activation of p53 in PSCs, which may be responsible for the apoptosis observed.

ATM and ATR are involved in the MNNG-induced phosphorylation of p53

Activation of p53 following DNA damage can result from direct phosphorylation by the phosphatidylinositol 3-kinase-related kinases (PIKKs) ataxia teleangiectasia mutated (ATM) (Banin, 1998;Canman, 1998) or ataxia teleangiectasia mutated and Rad3 related

Figure 2-7.

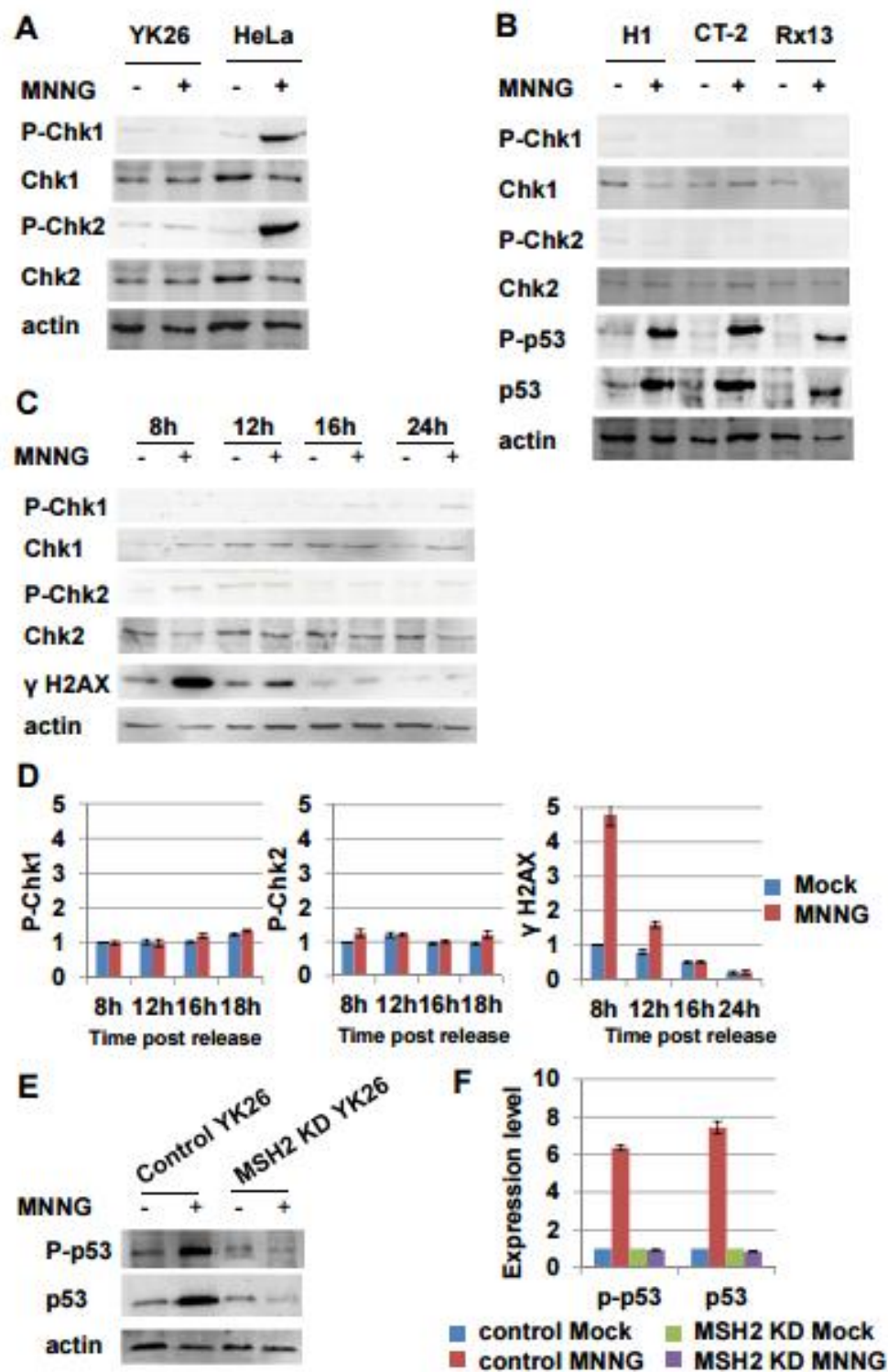


Figure 2-7. Chk1 and Chk2 are not activated in induced pluripotent stem cells in response to MNNG, but p53 is.

A, Western blot analysis of phospho-Chk1, phospho-Chk2, total Chk1 and total Chk2 in HeLa and YK26 cells with or without 2 μ M MNNG treatment for 24 hours. B, Western blot analysis of phospho-Chk1, phospho-Chk2, total Chk1, total Chk2, phospho-p53 and total p53 in H1, CT-2 and Rx13 cells with or without 2 μ M MNNG treatment for 24 hours. C, Western blot analysis of phospho-Chk1, phospho-Chk2, total Chk1, total Chk2 and γ H2AX in YK26 cells originally synchronized in mitosis with nocodazole then, with or without a 4 hour treatment of 2 μ M MNNG, harvested at different time points after release. D, Quantitation of Western blots represented in C. The values represent the means of three independent experiments. E, Western blot analysis of phospho-p53 (Ser15) and total p53 in control or MSH2 knockdown YK26 cells with or without 2 μ M MNNG treatment for 24 hours. Actin is included as a loading control. F, Quantitation of Western blots represented in E. The values represent the means of three independent experiments.

(ATR) (Tibbetts, 1999). To test whether these PIKKs were involved in the response to alkylation damage, we first examined MNNG treated YK26 and H1 cells for the presence of Ser 1981 phosphorylation of ATM (Bakkenist, 2003) and Ser 428 phosphorylation of ATR (Liu, 2011) as markers for DNA damage-dependent activation. We found that both ATM and ATR are phosphorylated following MNNG treatment of PSCs (Fig. 2-8A). ATR phosphorylation is similar to that observed in HeLa cells, however, ATM phosphorylation is not as enhanced in PSCs as HeLa. We next asked whether inhibiting the activity of ATM or ATR affected p53 induction and phosphorylation. We treated H1 cells with the ATM-specific inhibitor KU55933 or the ATR-specific inhibitor VE-821 along with MNNG for 24 hours and found that treatment with both inhibitors led to a partial reduction in the levels of damaged-induced total and phosphorylated p53 (Fig. 2-8B). When combining both inhibitors, we saw an additive effect as the levels of p53 activation were reduced even further than with either single agent alone. However, complete inhibition of p53 induction or phosphorylation was never observed which may suggest other kinases, such as DNA-PK, may be involved.

Figure 2-8.

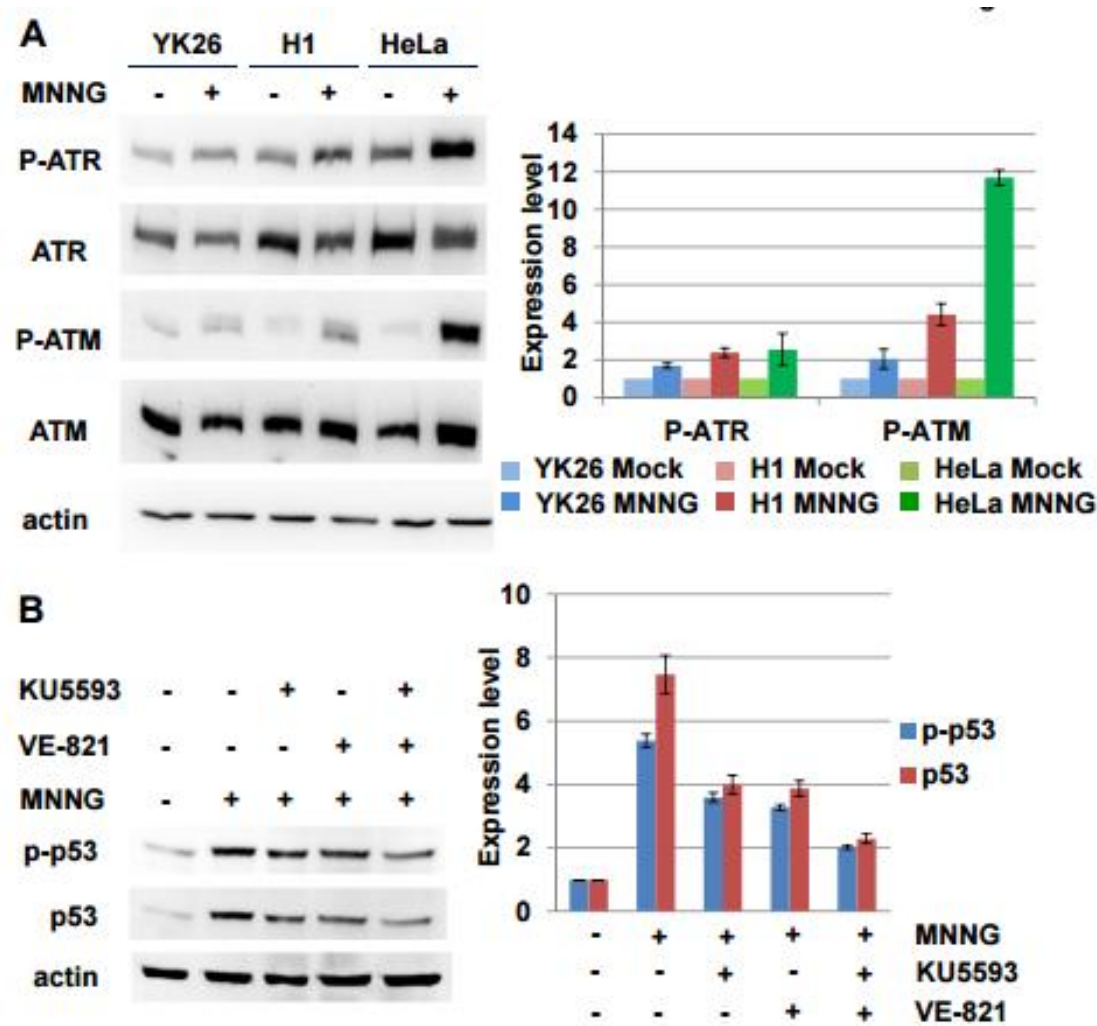


Figure 2-8. MNNG treatment leads to phosphorylation of ATR and ATM in pluripotent stem cells.

A, Western blot analysis of phospho-ATM (Ser 1981), phospho-ATR (Ser 428), total ATM and total ATR in H1, YK26 and HeLa cells with or without 2 μ M MNNG treatment for 24 hours. (Experiment performed by Dipika Gupta.) B, Western blot analysis of phospho-p53 and total p53 in H1 cells treated with 2 μ M MNNG and the ATM-specific inhibitor KU5593 or the ATR-specific inhibitor VE-821 or both for 24 hours. The values represent the means of three independent experiments.

E. DISCUSSION

Our results show that PSCs including both iPSCs and ESCs have a robust MMR pathway to protect the stability of their genome. Expression of the four major MMR proteins is greatly enhanced compared to primary fibroblasts from which our iPSCs were derived and slightly enhanced compared to rapidly dividing HeLa cancer cells. This is consistent with the upregulation of other DNA repair factors observed in PSCs compared to more differentiated cell types. Increased expression of factors involved in homologous recombination repair (HRR) such as RAD51 and BRCA1, non-homologous end joining such as Ku70 and base excision repair (BER) such as UNG and FEN1 has been reported in PSCs (Maynard, 2008; Momcilovic, 2010; Fan, 2011). The enhanced expression of DNA repair proteins in PSCs may underlie the increased repair efficiency observed in these cells. PSCs display accelerated repair of cyclobutane pyrimidine dimers caused by ultraviolet (UV) radiation, suggesting an enhanced nucleotide excision repair pathway (Luo, 2012; Maynard, 2008). Repair of modified bases caused by treatment with hydrogen peroxide or dimethyl sulfate is improved in PSCs compared to somatic cell types, suggesting enhanced BER (Luo, 2012; Maynard, 2008). Double strand breaks caused by hydrogen peroxide or gamma irradiation are repaired more efficiently in PSCs than in somatic cells (Adams, 2010; Luo, 2012; Maynard, 2008; Fan, 2011). Similarly, we detected high levels of single base pair mismatch correction by the MMR pathway in iPSCs and ESCs. Thus, the enhancement of DNA repair pathways appears to be an important strategy that PSCs employ to protect their genome.

However, increased expression of repair factors may not always promote increased DNA repair. The levels of MMR proteins expressed in PSCs were slightly higher than in HeLa cells, yet the repair activity in PSCs was slightly reduced compared to the cancer cells. These results may suggest that at the high expression levels observed in both PSCs and HeLa cells, the amounts of the four major MMR proteins are no longer rate limiting in the repair process. Localization of the MMR proteins to the mismatched template or the availability of other proteins involved in repairing the mismatch may be limiting. Alternatively, as 80% or more of the transfected mismatched template are repaired in PSCs, we may be reaching the limitations of the assay to discern repair efficiency.

Another important strategy used by PSCs to prevent mutation is an increased hypersensitivity to DNA damage. Increased apoptosis has been observed in PSCs treated with a variety of DNA damaging agents including UV (Luo, 2012; Qin, 2007), gamma irradiation (Wilson, 2010; Momcilovic, 2010; Fillion, 2009; Fan, 2011), cisplatin (Desmarais, 2012) and thymidine (Desmarais, 2012). Our results show that PSCs undergo massive apoptosis in response to the alkylating agent MNNG. Interestingly, Figure 2-4B also reveals an increased level of background apoptosis in untreated iPSCs compared to MMR knockdown iPSCs. These results may suggest sensitivity to even endogenously-generated DNA damage in a MMR-dependent manner. Alternatively, the high proliferation rate of PSCs may increase mismatch formation which, if a certain threshold is reached, may result in replication stress due to the excessive MMR activity. As PSCs are particularly sensitive to replicative stress (Desmarais, 2012), this may lead

to increased cell death. While such a mechanism has not been described in somatic cells, yeast displaying a mutator phenotype due to mutations in polymerase δ have been shown to have prolonged S-phase and evidence of a G₂/M arrest consistent with replication stress signals due to increased mutation generation (Venkatesan, 2006).

Whereas somatic cell types have also been shown to be sensitive to MNNG in a MMR dependent fashion, we show here that the commitment to cell death occurs much more quickly in PSCs. Somatic cells treated with MNNG require two rounds of S-phase following treatment resulting in a G₂/M arrest and, eventually, cell death. Why two cell cycles are necessary is not entirely clear, however, the futile cycle model suggests that MMR processing of MeG–T mismatches in the first S-phase results in persistent unreplicated gaps that are converted to lethal double strand breaks in the second S-phase (Fig. 2-9). One potential implication is that the two cell cycles provide an increased opportunity to resolve the primary MeG lesion. For example, cells suffering low levels of MeG damage may be protected against its mutagenic effects by the MMR pathway until MGMT is able to remove the MeG lesion. Repair of the unreplicated region caused by MMR processing at a later time point would allow the cell to ultimately survive. Accumulating evidence suggests that somatic cells are capable of exiting S-phase with incompletely replicated chromosomes and may be able to repair these regions during the subsequent cell cycle (Mankouri, 2013). Cells undergoing replicative stress are marked in the following G₁-phase by large, 53BP1 foci that may play a role in shielding unreplicated gaps until they can be repaired during the next S-phase (Harrigan, 2011; Lukas, 2011). Even if the unreplicated regions go unrepaired and are converted

to double strand breaks, the breaks could be a substrate for HRR, again leading to cell survival. Consistent with this model, depletion of the HRR protein Rad51d in mouse embryonic fibroblasts resulted in a fivefold increased sensitivity to MNNG compared to wild-type cells (Rajesh, 2010). This increased sensitivity was alleviated when MLH1 was also depleted, indicative of HRR playing a role in resolving secondary damage generated by MMR-lesion processing. The immediate apoptotic response observed in PSCs suggests that these cells do not have any extra time to resolve the alkylation damage.

One possibility that will require further investigation is that PSCs, unlike somatic cells, cannot tolerate perturbed S-phase progression such as might occur during futile cycles of MMR (Fig. 2-9). PSCs have already been shown to lack intra-S phase checkpoints in response to replication stress that normally function to stabilize replication forks and allow for replication re-start (Desmarais, 2012). In the current study, we observed a similar failure of PSCs to activate Chk1 in response to MNNG, thus missing a possibly important signaling pathway by which somatic cells survive MMR processing of MeG–T mismatches in the first S-phase (Noonan, 2012). Therefore, the futile MMR cycling at MeG–T mismatches may result in replication stress through either stalled polymerase forks or the generation of unreplicated single-stranded gaps that lead to immediate apoptosis induction. Interestingly, we do see an increase in γ -H2AX activation in the first S-phase after damage which has been associated with increased replication stress (Sirbu, 2011). Alternatively, the MMR proteins may be functioning through a direct signaling mechanism to recruit stress response proteins to the sites of damage. We

Figure 2-9.

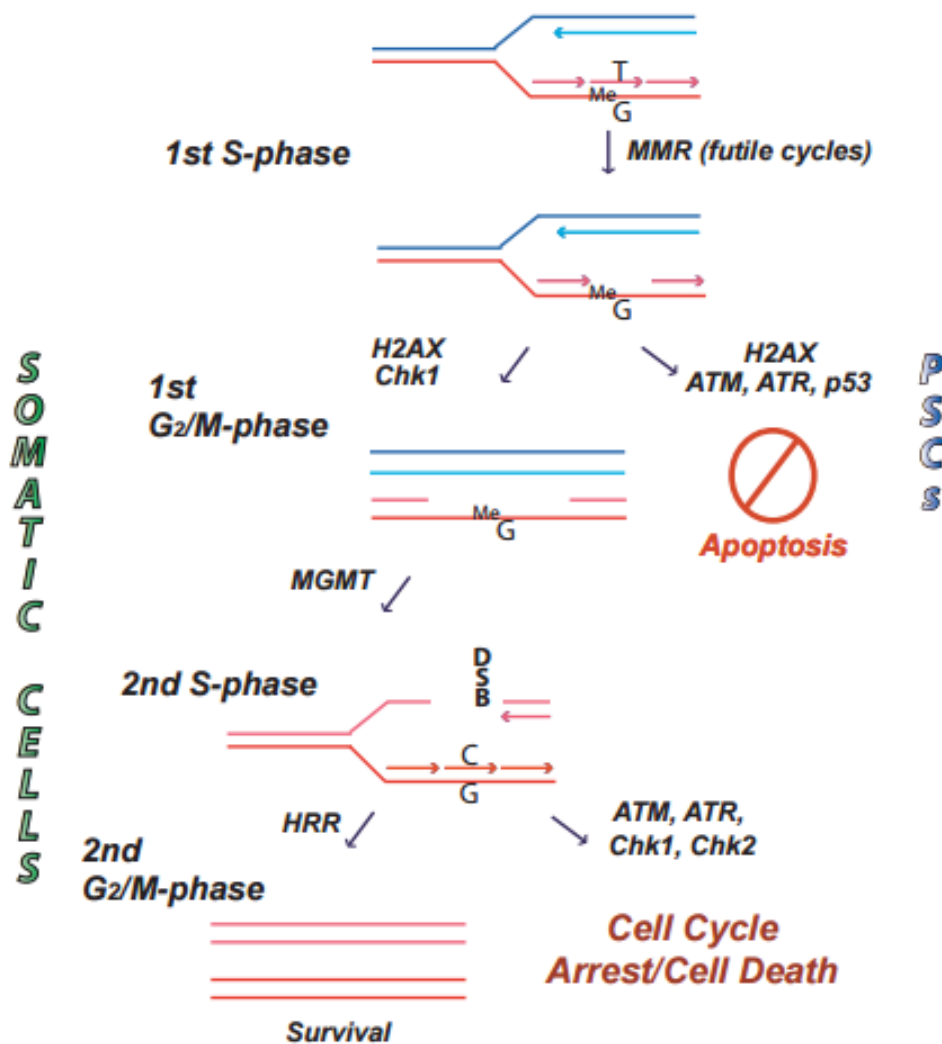


Figure 2-9. Model of the mismatch repair-dependent damage response to alkylation damage in somatic cells versus human pluripotent stem cells. Details described in text.

have shown that MNNG results in the phosphorylation of ATM and ATR as well as the MMR-dependent stabilization and activation of p53, which unlike in somatic cells (Noonan, 2012), leads to cell death during the first S-phase in PSCs. The explanation for this differing outcome between cell types may come from recent data showing that ESCs have an enhanced mitochondrial readiness for apoptosis compared to more differentiated cell types (Liu, 2013). Although p53 activation is similar between ESCs and differentiated cells following treatment with the radiomimetic drug neocarzinostatin, the balance of pro- and anti-apoptotic proteins in ESCs is such that they are more prone to undergo apoptosis.

Our results raise interesting questions about the molecular pathways involved in the apoptotic response to MNNG in PSCs. Both ATM and ATR are involved in activating p53. Inhibiting both kinases reduces the level of p53 activation, though it does not eliminate p53 activation entirely. Whether the increased activation of p53 by multiple kinases is required to induce an apoptotic response or whether the overlap provides a fail-safe mechanism to ensure p53 activation and apoptosis upon damage is not clear. In addition, it is not clear why ATM and ATR activation are not accompanied by activation of Chk1 and Chk2. Determining whether Chk1 and Chk2 are prevented from being phosphorylated by the PIKKs or whether they are phosphorylated and rapidly turned over is an important mechanistic question for determining how PSCs respond to replicative stress.

Understanding the mechanisms by which PSCs handle genotoxic stress will be extremely important if these cells are to realize their full potential as therapeutic agents in regenerative medicine. In addition, our results may provide insight into the role of the MMR pathway in preventing tumorigenesis. An important question that our studies raise is whether adult stem cells and cancer stem cells behave more like PSCs with regard to their MMR-damage response or more like differentiated cells in culture. If they are similar to PSCs, the increased sensitivity to DNA damage may result in a strong selection pressure for loss of MMR function. We have previously proposed that colonic stem cells from Lynch syndrome patients, which are heterozygous for a given MMR gene, may be under selection pressure to lose the remaining wild-type allele when exposed to DNA damaging agents in the colonic environment, thus enhancing tumorigenesis (Heinen, 2002). The damage response mechanism may also have implications for tumor response to therapy. If cancer stem cells do not share the same rapid apoptotic response to damage with PSCs, it is possible that their response may be made more similar to PSCs by priming the cells for apoptosis through the use of antiapoptotic protein inhibitors (Liu, 2013). More studies will be required to better understand the MMR damage response in multiple cell types, however, our results reveal the utility of using PSCs for drug response testing.

CHAPTER 3

The Use Of Human Intestinal Organoids To Study The Effects Of Early Cancer-Causing Mutations On intestinal Stem Cells

A. ABSTRACT

Lynch syndrome is a hereditary disease predisposing patients to colorectal and other cancers, caused by germline mutations in DNA mismatch repair (MMR) genes. How loss of MMR contributes to cancer is still unclear. The MMR pathway preserves genome fidelity following DNA replication and induces apoptosis and cell cycle arrest in cancer cells in response to DNA damage. We tested how this MMR-dependent damage response affects normal human intestine using human intestinal organoids and found that intestinal cells undergo not only apoptosis, but also a novel senescence response and accelerated differentiation in a MMR-dependent manner following alkylation damage. The cells undergoing apoptosis are primarily the intestinal stem cells suggesting different cell types in the intestine have different responses to damage. Together these results indicate that loss of MMR function in the intestinal crypts may provide a selective advantage that contributes to tumorigenesis particularly in the context of increased DNA damage.

B. INTRODUCTION

Lynch syndrome (LS) is a hereditary syndrome predisposing patients to a spectrum of cancers, primarily colorectal cancer (CRC) (Lynch et al., 2015). With a > 80% lifetime risk of developing CRC, these patients would benefit from improved prevention measures such as chemoprevention, though chemopreventative strategies for LS patients to date have been largely unsuccessful (Ricciardiello et al., 2016). An improved understanding of how intestinal cells are impacted by early cancer-causing mutations would aid such an effort. An early change in LS CRC is loss of DNA mismatch repair (MMR) function. LS is caused by germline mutations in one copy of a DNA MMR gene (Lynch et al., 2015). Cancer development is preceded by somatic loss of the remaining wild-type allele most likely in an intestinal stem cell (ISC) which is thought to be the cell of origin of CRC (White and Lowry, 2015). How loss of MMR function contributes to tumorigenesis is still not entirely clear. The MMR pathway repairs mistakes made by the DNA polymerase during replication with MMR loss increasing the mutation rate nearly 1,000-fold (Kolodner, 1996; Modrich, 1991; Strand et al., 1993). Thus, MMR-defective cells develop a mutator phenotype that increases the risk of mutation in other important oncogenes and tumor suppressors (Fishel and Kolodner, 1995). In addition, the MMR pathway is involved in inducing apoptosis and cell cycle arrest in cancer cell lines in response to certain DNA damaging agents (Li et al., 2016; Stojic et al., 2004). Whether this response is active in normal human intestinal cells and plays a role in tumor suppression is an important unanswered question as a suitable model system for studying the effects of cancer-causing mutations on human intestinal cells is lacking.

The recent development of three-dimensional human tissue organoids may provide a powerful new model for answering this question. Human intestinal organoids (HIOs) have been created from intact intestinal crypts as well as through the directed differentiation of human embryonic stem cells (hESCs) (Cao et al., 2011; Sato et al., 2011; Spence et al., 2011). HIOs are self-renewing and display markers of differentiated intestinal epithelium suggesting that they recapitulate the different cell types found in the human intestine. Here, we have used wild-type and MMR-knockout hESCs as well as adult colon tissue to create HIOs for studying the MMR-dependent damage response to DNA alkylation damage in normal human intestinal cells. We find that different intestinal cell types undergo different MMR-dependent responses to DNA damage.

C. MATERIALS AND METHODS

Differentiation of hESC-derived HIOs

H1 hESCs were maintained on Matrigel-coated tissue culture plates in hESC media. hESCs were differentiated into HIOs as previously described (McCracken et al., 2011) except for addition of 6 μ M of the GSK3 β inhibitor CHIR99021 to definitive endoderm cells to form hindgut spheroids. Briefly, H1 ESCs were differentiated to definitive endoderm (DE) by addition of Activin A (100 ng/ml; R&D Systems) for three days in RPMI 1640 media (Gibco) containing increasing concentrations (0%, 0.2%, and 2.0%) of defined fetal bovine serum (dFBS). Following DE induction, cells were cultured in DMEM/F12 media (Lonza) with B27 (Invitrogen) and the GSK3 β inhibitor CHIR99021 (6 μ M; Selleck Chemicals) for 4 days to form hindgut spheroids. The media was

changed every day. Spheroids were collected, resuspended in 50µl Matrigel (BD Biosciences), and plated in a three-dimensional droplet. After Matrigel was allowed to solidify for 10–15 minutes in a tissue culture incubator, spheroids were overlaid with HIO media: DMEM/F12 with B27, EGF (100ng/ml; R&D Systems), noggin (100ng/ml; R&D Systems) and R-spondin1 (500ng/ml; R&D Systems). Media was replaced every 3 days. Following 2 weeks, HIOs were collected and re-plated in fresh Matrigel at a dilution of 1:6.

MSH2 Knockout in hESCs

MSH2 knockout hESCs were derived using CRISPR/Cas9 gene editing with a guide RNA targeting the first exon of *MSH2*. Briefly, the guide RNA was cloned into the Px459V2.0 vector. H1 hESCs were treated with 10 µM ROCK inhibitor Y-27632 (Selleck Chemicals) for 2h before nucleofection. One million cells were nucleofected (Amaxa2b, program B-016) with 2µg of the vector DNA expressing the guide RNA, the Cas9 cDNA and a puromycin resistance gene. Transfected cells were selected with 0.5µg/mL puromycin starting 24h after nucleofection for 2 days. After 2 days of selection, fresh medium was added daily and the single cell clones were picked 12-15 days later. Single cell clones were screened via Hot Shot DNA isolation and PCR and restriction enzyme analysis to determine disruptions near the target site. Clones identified with a positive PCR screen were verified by genomic DNA sequencing as well as by Western blot to check for loss of MSH2 protein expression.

Generation of LGR5-eGFP HIOs

The LGR5-eGFP BAC, kindly provided by Dr. Jason Spence (McCracken et al., 2014), was nucleofected into single cell suspensions of H1 hESCs using the Amaxa Human Stem Cell Nucleofector Starter Kit. Cells were grown in G418 (200µg/ml) for two weeks to select for cells that took up the BAC. G418-resistant H1 ESCs were maintained in antibiotic indefinitely. LGR5-eGFP H1 ESCs were differentiated into HIOs as described above. Live images of LGR5-eGFP HIOs were obtained using a Lightsheet Z.1 fluorescence microscope (Zeiss).

Creation of adult HIEs

Surgically resected normal colon tissue samples from de-identified patients were obtained from the UConnHealth Tissue Biorepository. The tissues were washed and stripped of the underlying muscle layers, then chopped into approximately 5mm pieces and further washed with cold PBS. Next, the tissue fragments were incubated and rocked in ice-cold 25 mmol/L EDTA buffer for 40 minutes in the cold room. After removal of the EDTA buffer, tissue fragments were vigorously resuspended in cold PBS by vortexing to isolate intestinal crypts. 6-8 repetitions of vortexing for 30 seconds were performed and supernatants were collected each time. Isolated crypts were pelleted, washed with cold PBS, and centrifuged at 200g for 3 minutes. The crypts were resuspended in Matrigel and plated. After Matrigel solidified at 37°C, adult enteroid media was overlaid containing DMEM/F12, B27, penicillin/streptomycin (Invitrogen), *N*-acetylcysteine (1mM; Sigma-Aldrich), gastrin (10nM; Sigma-Aldrich), nicotinamide (10mM; Sigma-Aldrich), A83-01 (500nM; Sigma-Aldrich), SB202190 (10µM; Sigma-

Aldrich), EGF (100ng/ml), noggin (100ng/ml), R-spondin1 (500ng/ml). Y-27632 (10 μ M) was added for the first 2 days. Media was changed every 2 days.

Immunofluorescent staining

HIOs or HIEs were harvested and Matrigel was removed by incubating with cold cell recovery solution for 1h before embedding into OCT. OCT sections were cut at 7 μ m, fixed with 10%NBF for 15 minutes and permeabilized with 0.5% Triton X-100. Sections were blocked with 5% BSA for 1h at room temperature followed by incubation with primary and secondary antibodies listed in Table 3-1. Where indicated, EdU (10 μ M) was added to the media for 48h before harvesting and imaged following the manufacturer's protocol (Thermo Scientific).

Cell viability assay in HIOs

Cell number in a well of HIOs was quantified by incubating with resazurin for 4h and measuring the emission spectra at 590 nm in a PerkinElmerEnSpire 2300 Multilabel Reader. HIOs were mock-treated or treated with 25 μ M O^6 -BG and the indicated concentrations of MNNG for 24, 48 or 72 h. The remaining live cells were quantified using the ApoLive-Glo viability assay according to manufacturer's instructions (Promega). The percentage of live cells was normalized to the initial number.

Senescence assays

Frozen sections of HIOs and HIEs were stained for SA- β gal activity according to the manufacturer's protocol (Cell Signaling Technologies). Briefly, sections were fixed at room temperature for 10 min in fixation solution. Sections were washed in PBS and incubated in X-gal solution at 37°C overnight. After washing with PBS, sections were mounted and visualized by light microscopy. For the conditioned medium assay, HIOs were mock-treated or treated with 25 μ M O^6 -BG and 2 μ M MNNG for 48h and changed to fresh medium for another 48h. The conditioned medium was added to primary human dermal fibroblasts for 48h followed by culturing in normal growth medium (DMEM+ 10%FBS) for an additional 48h before performing the SA- β gal assay.

RT-PCR in HIOs

HIOs were harvested by incubation with TrypLE (Invitrogen) for 5 minutes at 37°C. RNA was isolated using the Nucleospin RNA kit according to the manufacturer's instructions (Macherey-Nagel). cDNA was synthesized using the Taqman RT kit (Thermo Scientific). qRT-PCR was performed using primers listed in Table 3-2. Relative quantification was achieved by normalizing an Actin gene control.

D. RESULTS

Differentiation of wild-type and MSH2 knockout hESCs into HIOs

To study the MMR-dependent response to DNA alkylation damage in normal human intestinal cells, we created HIOs through directed differentiation of H1 hESCs following a three-step protocol previously described (Hannan et al., 2013; Spence et al., 2011) (Figure 3-1A). Differentiation into definitive endoderm cells and then hindgut cells was marked by expression of the transcription factors Sox17 and CDX2, respectively (Figure 3-1B). Clusters of hindgut spheroids were placed into a three-dimensional culture in Matrigel to form HIOs which grew steadily over several weeks (Figure 3-1C). The HIOs displayed a single-layer of epithelial cells and a surrounding mesenchymal layer as described previously (Spence et al., 2011) (Figure 3-1D). The HIOs expressed multiple intestinal markers including CDX2, E-cadherin and markers of differentiated intestine such as mucin and villin (Figure 3-1E). The major MMR proteins were expressed in HIOs though at reduced levels compared to H1 hESCs where they are highly expressed (Lin et al., 2014) (Figure 3-2A). Two week-old HIOs expressed the MMR proteins MSH2 and MLH1 in the majority of cells coinciding with a high number of proliferating cells as determined by incorporation of the thymidine analog Ethynyl-2'-deoxyuridine (EdU) (Figure 3-2B). To determine the effects of MMR loss on intestinal cells, we knocked out the *MSH2* gene in hESCs using the Clustered Regularly Interspaced Short Palindromic Repeats (CRISPR)-Cas9 gene editing system (Figure 3-2C and 3-2D) prior to differentiation into HIOs. Knockout of both alleles of *MSH2* led to complete loss of MSH2 protein expression in hESCs (Figure 3-2E) and in subsequent HIOs (Figure 3-2F).

Figure 3-1.

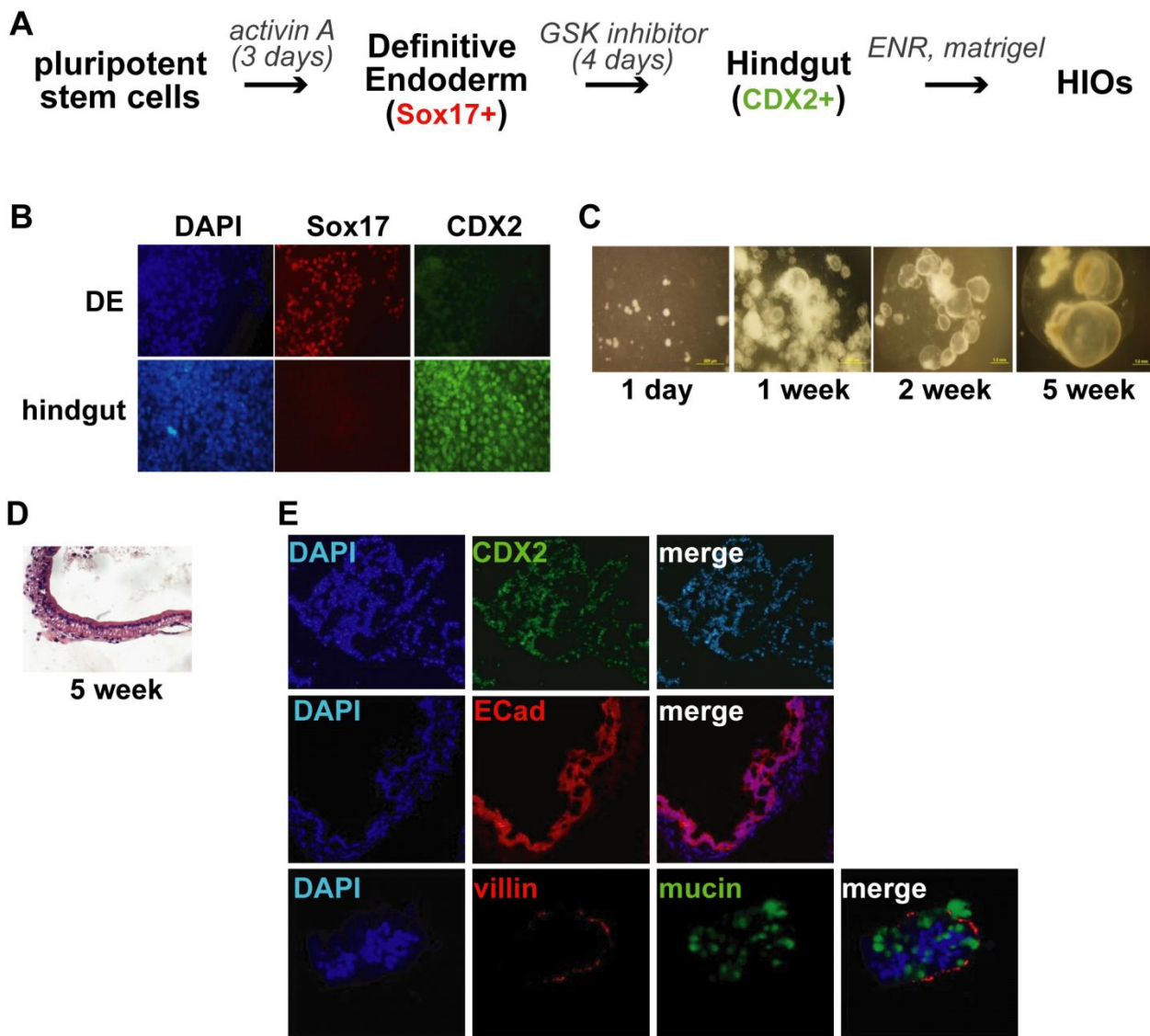


Figure 3-1. Generation of HIOs from hESCs.

- (A) Schematic of the protocol to differentiate hESCs into HIOs
- (B) Immunofluorescent staining of markers for differentiated endoderm (DE) and hindgut cells.
- (C) Bright field images of HIOs embedded in Matrigel at various time points.
- (D) Hematoxylin and eosin staining of a section from a 5 week old HIO.
- (E) Immunofluorescent staining displaying the expression of the intestinal transcription factor CDX2, the epithelial cell marker E-cadherin or the intestinal differentiation markers villin and mucin in HIOs.

Figure 3-2.

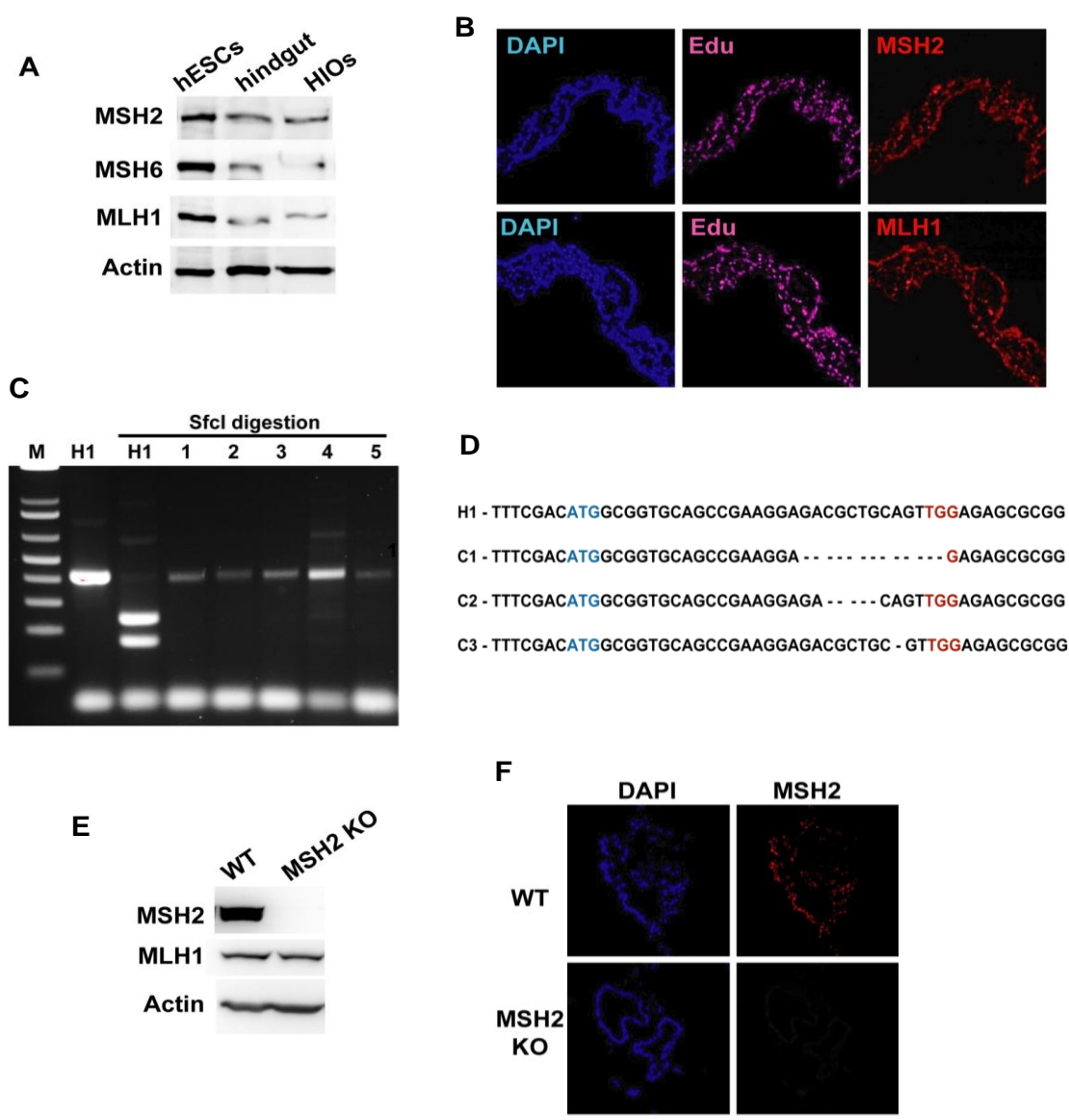


Figure 3-2. MSH2 expression and knockout in HIOs

(A) Western blot analysis of the major MMR proteins in hESCs, hindgut cells and HIOs.

(B) Immunofluorescent (IF) staining of 2 week old HIOs for MSH2 and MLH1 and EdU incorporation to identify dividing cells.

(C) SfcI digestion of exon 1 of *MSH2* PCR products from H1 hESCs or individually targeted clones. Successful targeting results in ablation of the SfcI site in either a homozygous (clones 1-3, 5) or heterozygous (clone 4) fashion. (MSH2 KO hESCs were generated by Dr. Abhijit Rath)

(D) Sequences of H1 hESCs and three homozygous MSH2 KO clones.

(E) Western blot analysis of MSH2 and MLH1 protein expression in wild-type (WT) and MSH2 knockout (KO) hESCs.

(F) IF staining of MSH2 in WT and MSH2 KO HIOs.

Alkylation damage leads to both MMR-dependent apoptosis and senescence

We tested the response of intestinal cells to DNA alkylation damage by treating wild-type or MSH2 knockout (KO) HIOs with the S_N1 alkylating agent *N*-methyl-*N'*-nitro-*N*-nitrosoguanidine (MNNG). Treatment of MMR-proficient cancer cell lines with MNNG results in a permanent G_2 arrest due to the creation of O^6 -methylguanine (O^6 -MeG) lesions (Li et al., 2016; Stojic et al., 2004). HIOs were pre-treated with the MGMT inhibitor O^6 -benzylguanine (O^6 -BG) to inhibit direct repair of O^6 -MeG lesions prior to addition of MNNG, and overall cell survival was monitored. Whereas hESCs show extensive cell death following 24 hours of treatment (Figure 3-S1), wild-type HIOs were much less sensitive to MNNG even at higher concentrations with longer exposure times (Figure 3-3A). To determine if any cells were undergoing apoptosis, we performed immunofluorescence experiments on frozen sections from mock or MNNG-treated HIOs using an antibody against cleaved-Caspase-3. We found an increase in cleaved-Caspase-3-positive cells in wild-type, but not in the MSH2 KO HIOs after MNNG treatment (Figure 3-3B). Our results indicate that MNNG treatment induces a MMR-dependent apoptotic response in intestinal cells within HIOs, but to a much lesser extent than in undifferentiated hESCs.

When examining proliferation in 2 week old HIOs, we noticed a dramatic reduction of EdU incorporation in wild-type HIOs treated with MNNG compared to mock-treated controls (Figure 3-3C and 3-3D). This reduction was not seen in MSH2 KO HIOs indicative of a MMR-dependent effect. In 5 week old HIOs, the overall amount of proliferation was reduced consistent with increased differentiation, yet treatment with

MNNG still yielded a further decline in proliferating cells (Figure 3-3D). Loss of proliferative capacity in the absence of extensive apoptosis led us to ask whether cells were senescing in response to MNNG. We found increased numbers of cells that were positive for senescence-associated β -galactosidase (SA- β gal) activity following 48 hours of MNNG treatment. This SA- β gal activity was not seen in MSH2 KO HIOs (Figure 3-3E). We observed senescent cells still present in the HIOs one week following treatment (Figure 3-3F) which suggests that in the absence of immunological clearing, the senescent cells persist and likely contribute to the unexpectedly high number of surviving cells following MNNG treatment seen in Figure 3-3A. As a MMR-dependent senescence response to damage had not been reported before, we checked whether senescence could be observed in MNNG treated HeLa cervical cancer cells or hESCs. We did not see any evidence of SA- β gal activity in either HeLa cells or H1 hESCs after MNNG treatment (Figure 3-3G).

A striking feature of senescent cells is a senescence-associated secretory phenotype (SASP) which involves the upregulation of matrix-degrading enzymes, cytokines and growth factors that when secreted can affect neighboring cells (Campisi and d'Adda di Fagagna, 2007). Using RT-PCR, we observed a subtle, but significant increase in the mRNA levels of SASP factors such as IL-6 and MMP3 in HIOs following MNNG treatment (Figure 3-3H). While the increase in expression levels is not dramatic, we attribute that to the fact that while cDNA is prepared from entire HIOs, only a small subset of the cells is actively senescing. To further test whether SASP is occurring in the treated HIOs, we took advantage of the fact that SASP can induce senescence in other cells in a paracrine fashion (Acosta et al., 2013). We found that conditioned

Figure 3-3.

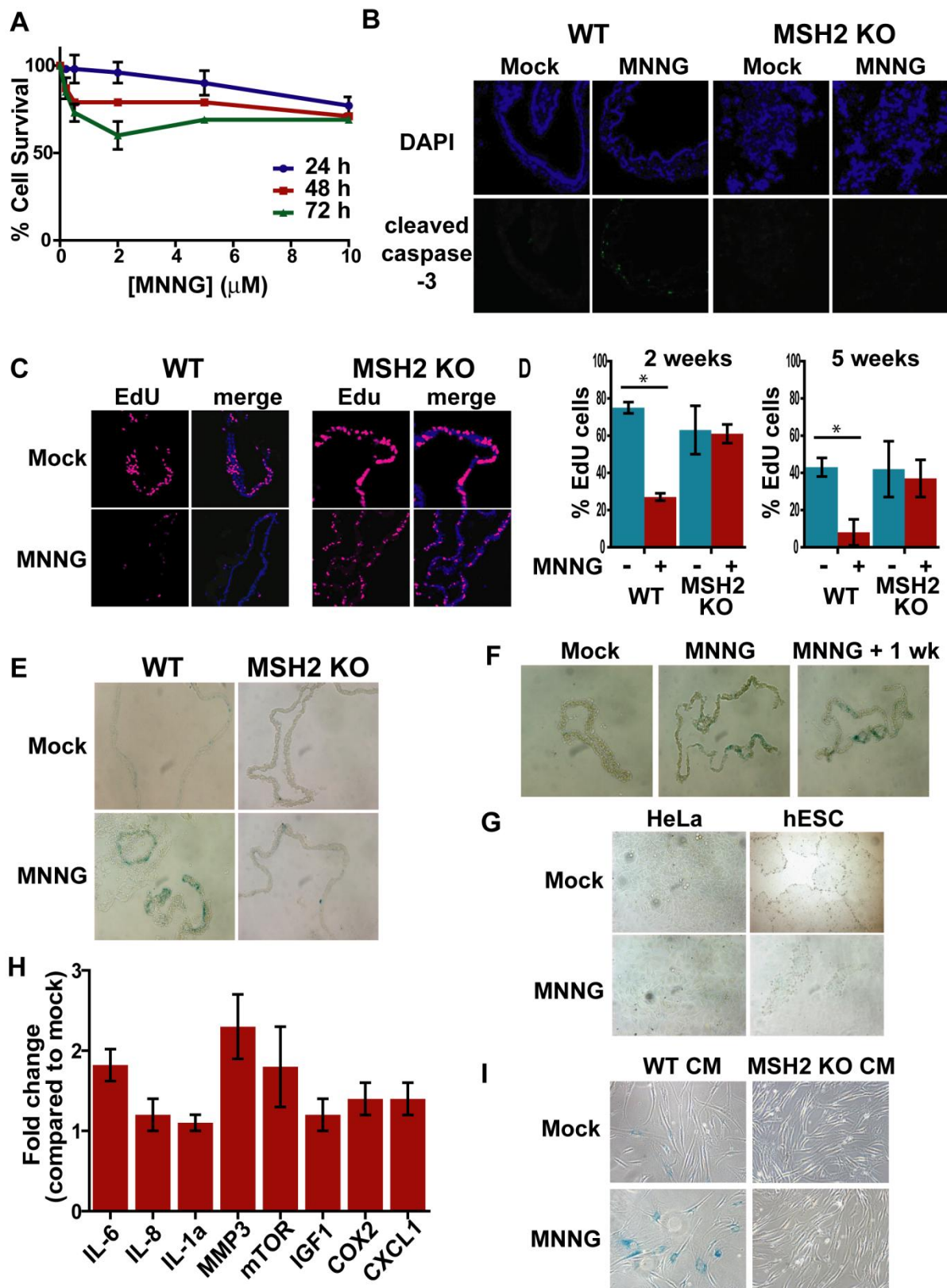


Figure 3-3. Alkylation damage leads to both a MMR-dependent apoptotic and senescent response

(A) Plot of cell survival of wild-type HIOs after MNNG treatment for 24, 48 or 72 hours.

Data correspond to the average of three independent experiments \pm SEM.

(B) Immunofluorescent (IF) staining of cleaved-caspase 3 in wild-type (WT) and MSH2 knockout (KO) HIOs after mock or 2 μ M MNNG treatment for 48hours.

(C) IF staining of EdU incorporation in WT and MSH2 KO HIOs after mock or 2 μ M MNNG treatment for 48hours.

(D) Quantification of EdU incorporation in 2 week and 5 week old WT and MSH2 KO HIOs with and without MNNG treatment. Statistical significance was assessed from three independent experiments by the two-tailed Student's t test: * $p < 0.05$.

(E) Senescence-associated beta-galactosidase (SA- β gal) staining of WT and MSH2 KO HIOs after mock or 2 μ M MNNG treatment for 48hours.

(F) SA- β gal staining of WT HIOs immediately after or 1 week after a 48 hour treatment with 2 μ M MNNG.

(G) SA- β gal staining of HeLa cells and hESCs after mock or 2 μ M MNNG treatment for 48hours and 24hours, respectively.

(H) RT-PCR of WT HIOs after mock or 2 μ M MNNG treatment for 48hours. Data correspond to the average of three independent experiments \pm SEM. Statistical significance was assessed by the two-tailed Student's t test: * $p < 0.05$.

(I) SA- β gal staining of primary fibroblasts after a 48 hour incubation with conditioned medium from WT and MSH2 KO HIOs that were either mock treated or treated with 2 μ M MNNG for 48 hours.

medium from MNNG-treated wild-type HIOs, but not from MSH2 KO HIOs, could induce senescence in primary human dermal fibroblasts (Figure 3-3I). Together, these results reveal a novel, MMR-dependent senescence response to DNA damage in intestinal cells.

The MMR-dependent apoptotic response to damage occurs in intestinal stem cells

We next explored the basis for the differential damage response observed in HIOs. We hypothesized that it may be dependent on the type of intestinal cell. Based on our observations that hESCs are prone to apoptosis (Lin et al., 2014), we posited that cells undergoing apoptosis were ISCs. To identify ISCs, we utilized a LGR5-eGFP reporter construct derived from a bacterial artificial chromosome (BAC) containing the LGR5 ISC marker gene (Barker et al., 2007) in which the initiator methionine was replaced with an eGFP cassette (McCracken et al., 2014). We stably transfected this BAC into hESCs prior to differentiation into HIOs. We observed widespread Lgr5-GFP expression in early stage HIOs, that became more isolated into smaller clusters of cells as the HIOs grew and matured (Figure 3-4A, 3-4B and 3-4C). LGR5-GFP positive cells actively proliferate as indicated by EdU labeling, though not every EdU labeled cell is GFP-positive suggesting that EdU labeling identifies both ISCs and the transient amplifying cells (Figure 3-4B). We then treated LGR5-GFP HIOs with MNNG and used the cleaved-Caspase-3 antibody to detect apoptotic cells. We found that the majority of apoptotic cells either colocalized or were immediately adjacent to a GFP-positive ISC suggesting

Figure 3-4.

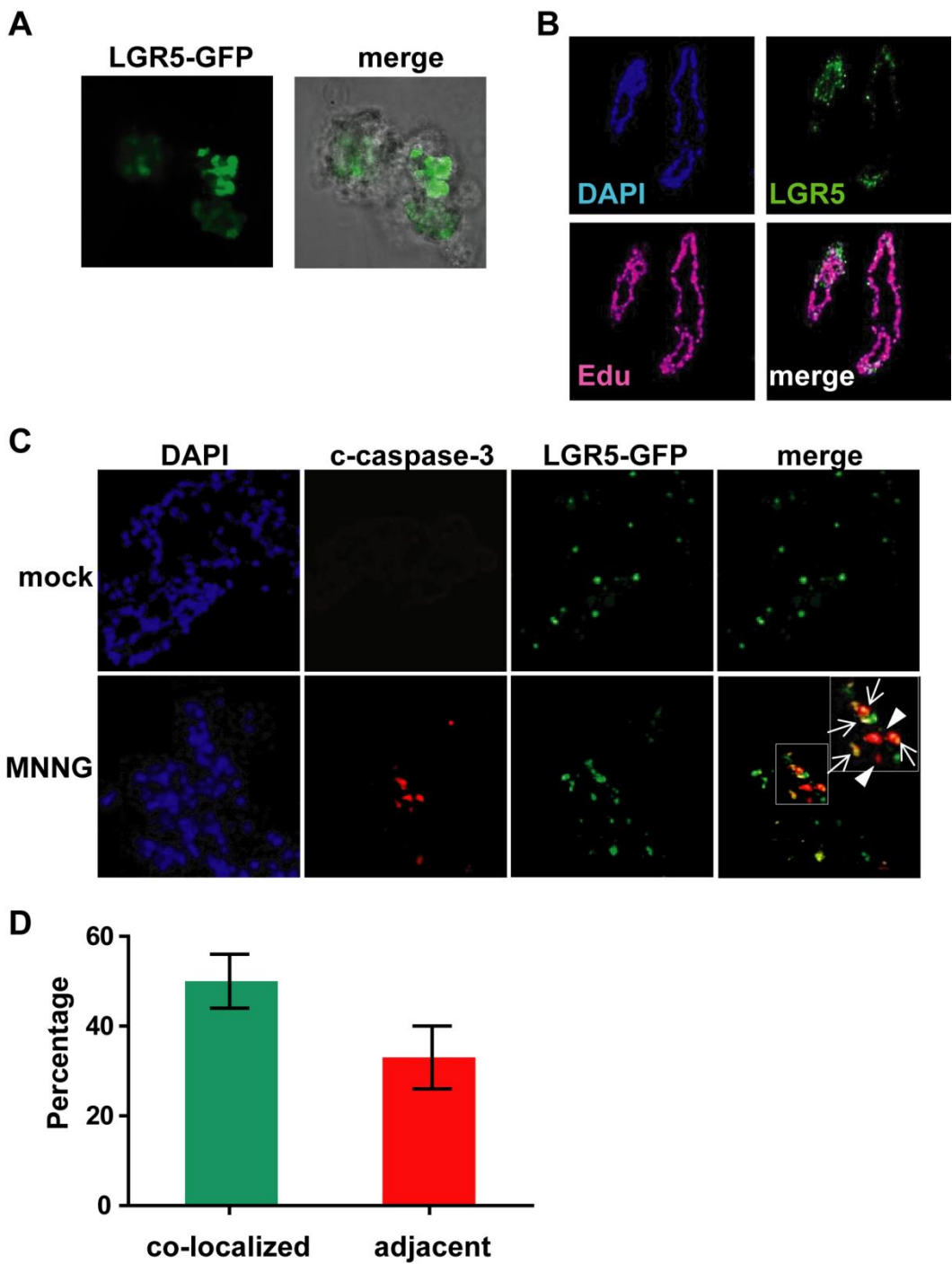


Figure 3-4. The MMR-dependent apoptotic response to damage occurs primarily in intestinal stem cells

(A) Light sheet fluorescence microscopy images of LGR5-GFP HIOs indicating the presence of intestinal stem cells.

(B) Immunofluorescent staining of 2 week old LGR5-GFP HIOs for GFP expression and EdU incorporation to identify dividing cells.

(C) Immunofluorescent staining of LGR5-GFP HIOs mock or MNNG treated showing GFP expression and cleaved-Caspase-3 (c-caspase-3) activation. Arrows indicate GFP+ cells that are co-localizing with cleaved-Caspase-3+ cells and arrowheads indicate those that are immediately adjacent.

(D) Quantification of co-localized or adjacent GFP and cleaved-Caspase-3 positive cells in 2 week old LGR5-GFP HIOs treated with MNNG. Data correspond to the average of three independent experiments \pm SEM.

that the cells undergoing apoptosis are most likely the ISCs or their immediate descendants (Figure 3-4C and 3-4D).

Adult intestinal enteroids show multiple responses to alkylation damage

While hESC-derived HIOs are a powerful tool for studying intestinal cell biology, expression profiles suggest these HIOs resemble more fetal-like tissue than adult intestine (Finkbeiner et al., 2015). We therefore wished to confirm that the novel damage response we were observing occurred in adult cells using HIOs derived from adult colon tissue, also referred to as human intestinal enteroids (HIEs). We obtained adult normal colon tissue from two de-identified patients, isolated the crypts and produced HIEs as described previously (Sato et al., 2011). We observed robust expression of the intestinal markers E-cadherin, mucin and villin (Figure 3-5A). In media containing exogenous EGF, noggin and R-spondin (ENR), the HIEs displayed limited proliferation and reduced survival likely due to loss of ISCs. Addition of the GSK3 β inhibitor CHIR99021, which has been shown to promote the survival and proliferation of ISCs in culture (Wang et al., 2013; Yin et al., 2014), enhanced proliferation of the HIEs. As the HIEs grew in the presence of CHIR99021, they displayed increased crypt budding and maintained this morphology even a week after withdrawing the inhibitor (Figure 3-5B). Consistent with the maintenance of a more progenitor cell-like phenotype, the HIEs in the presence of the inhibitor failed to display markers of terminal differentiation (Figure 3-5C, upper row). However, this effect was reversible as differentiated cell types re-appeared upon removal of the inhibitor from the medium

(Figure 3-5C, lower row). To determine if the HIEs were capable of mounting a senescence response to alkylation damage, we treated HIEs grown in the standard ENR media or in the presence of the GSK3 β inhibitor or in the presence of the inhibitor for 7 days followed by removal for 2 days with MNNG and examined SA- β gal activity. Interestingly, the MNNG-treated HIEs in the presence of the GSK3 β inhibitor did not have any senescent cells after treatment (Figure 3-5D, middle column). However, HIEs that were never treated with the GSK3 β inhibitor or in which the inhibitor was withdrawn both displayed senescent cells following MNNG treatment (Figure 3-5D, left and right columns). We next measured apoptosis in HIEs following MNNG treatment in the presence of the GSK3 β inhibitor or after withdrawal. We detected apoptotic cells only in the presence of the inhibitor (Figure 3-5E). Taken together, these results are consistent with an apoptotic response occurring primarily in ISCs following DNA damage whereas more differentiated cells likely senesce. In addition to apoptosis, we noticed that MNNG treatment resulted in the appearance of terminally differentiated cells in HIEs grown with the GSK3 β inhibitor, indicating that in adult tissues, a third response to alkylation damage is induced differentiation (Figure 3-5F).

Figure 3-5.

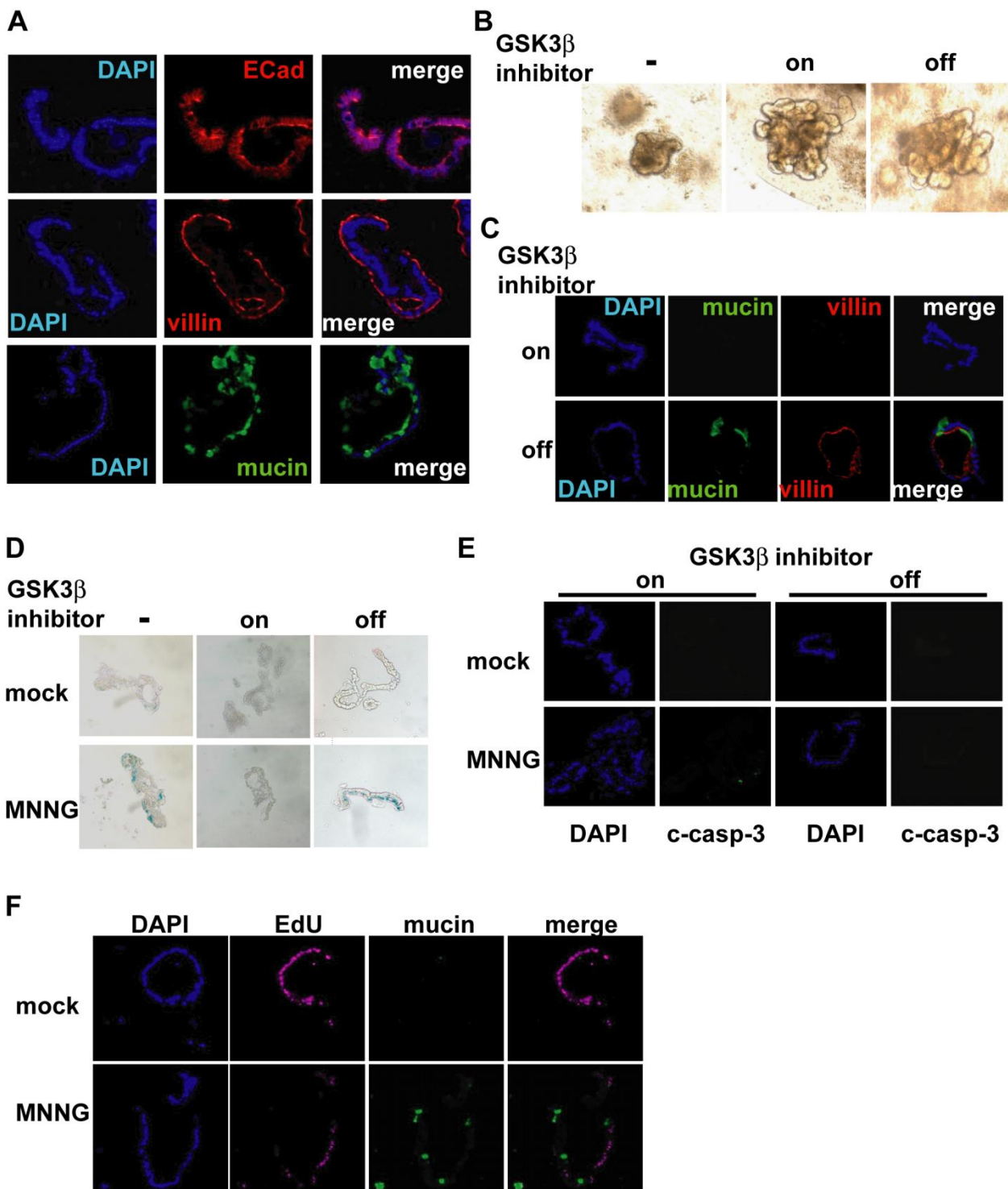


Figure 3-5. Adult human intestinal enteroids display both apoptotic and senescent responses to alkylation damage.

(A) Immunofluorescent (IF) staining of adult human intestinal enteroids (HIEs) showing expression of the epithelial cell marker E-cadherin or the differentiated intestinal cell markers villin and mucin.

(B) Bright field images of 5 day old adult HIEs in the absence (-) or presence (on) of GSK3 β inhibitor CHIR99021 or following its removal for 4 days (off).

(C) IF staining of mucin and villin in HIEs in the presence of the GSK3 β inhibitor (on) or 4 days following its removal (off).

(D) Senescence-associated beta-galactosidase staining of HIEs in the absence (-), presence (on) or 4 days following the removal of (off) the GSK3 β inhibitor after mock or MNNG treatment for 48hours.

(E) IF staining of cleaved-Caspase-3 (c-Casp-3) in HIEs in the presence of the GSK3 β inhibitor (on) or 4 days following its removal (off) and after mock or MNNG treatment for 48hours.

(F) IF staining for mucin and EdU incorporation in HIEs in the presence of the GSK3 β inhibitor after mock or MNNG treatment.

Figure 3-S1

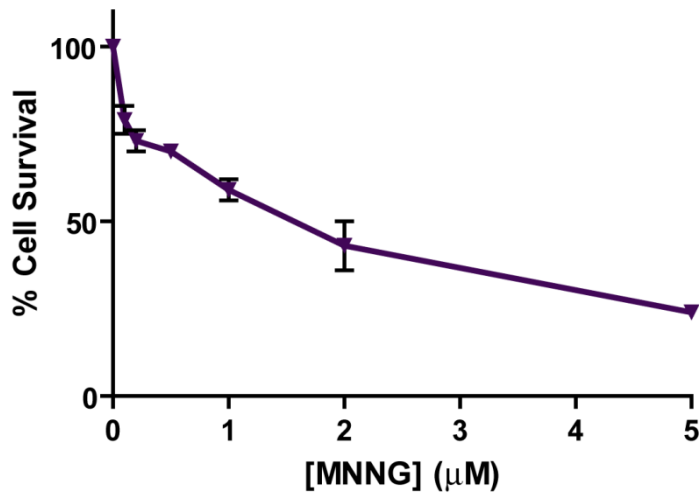


Figure 3-S1. Cell survival of hESCs after MNNG treatment.

Plot of cell survival of wild-type hESCs after MNNG treatment at different concentrations for 24 hours. Data correspond to the average of three independent experiments \pm SEM.

Table 3-1. Antibodies used for immunofluorescence staining

REAGENT or RESOURCE	SOURCE	IDENTIFIER	DILUTION
Antibodies			
Anti- cleaved-caspase-3	BD Biosciences	Cat No. 559565	1:100
Anti- MSH2	BD Biosciences	Cat No. 556349	1:100
Anti-MLH1	BD Biosciences	Cat No. 554073	1:100
Anti-GFP	Abcam	Cat No. ab13970	1:100
Anti-E-cadherin	BD Biosciences	Cat No. 610181	1:100
Anti-mucin	Santa Cruz Biotechnology	Cat No. sc-15334	1:200
Anti-villin	Santa Cruz Biotechnology	Cat No. sc-58897	1:200
Anti-Sox17	Abcam	Cat No. ab84990	1:100
Anti-CDX2	Abcam	Cat No. ab76541	1:100
Alexa Fluor 488	Molecular Probes	Cat No. A11034	1:200
Alexa Fluor 594	Molecular Probes	Cat No. A11032	1:200
Alexa Fluor 555	Thermo Scientific	Cat No. A-21437	1:200

Table 3-2. RT-PCR primers

Gene	Forward (5' to 3')	Reverse (5' to 3')
Actin	AGA GCT ACG AGC TGC CTG AC	AGC ACT GTG TTG GCG TAC AG
IL-6	TGA AAA AGA TGG ATG CTT CCA AT	TAC TCA TCT GCA CAG CTC T
IL-8	GCA GAG CAC ACA AGC TTC TAG G	CAA GAG AGC CAC GGC CA
IL-1a	TGA AAT AGT TCT TAG TGC CG	TTC TAA GAA TCT CAA AAA CTC AAT TG
MMP3	ATA TCA TCT TGA GAC AGG CG	TTG ATG ATGATG AAC AAT GGA C
mTOR	AGC CTC CAG TTC AGC AAG G	ATG GCA ACT ACA GAA TCA CAT GCC
IGF1	ACA AAC ACT TCC TTC CCT TC	ACT GAG GAC CTC GGA AT
COX2	TTG TAG CCA TAG TCA GCA TTG	AAT TAT TTC TGA AAC CCA CTC C
CXCL1	GCC ACA CTC AAG AAT GGG C	TCC TCC CTT CTG GTC AGT TG
p16	ATG GAG CCT TCG GCT GAC T	GTA ACT ATT CGG TGC GTT GGG

E. DISCUSSION

Collectively, our data suggest multiple MMR-dependent responses to DNA damage in different intestinal cell types in human HIOs and HIEs including a novel senescence response. ISCs appear more prone to undergo apoptosis in response to DNA damage; whereas, more differentiated cells such as the transient amplifying cells likely senesce. Both mechanisms may play an important role in tumor suppression in a cell-autonomous fashion by eliminating or halting progression of damaged cells themselves. However, senescence can play an important role in tumor suppression in non-autonomous ways as well. Through SASP activation, senescent cells can have effects on neighboring cells *in vivo*. The generation of an inflammatory response that can clear both the senescent cell but also neighboring malignant and pre-malignant cells may reduce tumorigenesis (Kang et al., 2011; Xue et al., 2007). In addition, SASP can induce senescence in other cells as we observed in Figure 3-3I which may spread this protective effect throughout a field of pre-malignant cells (Acosta et al., 2013).

However, senescence may be an imperfect tumor suppressing mechanism since it can promote tumorigenesis in some cases. SASP factors have been shown to promote proliferation of preneoplastic epithelial cells (Bavik et al., 2006; Krtolica et al., 2001) as well as stimulate angiogenesis and tumor invasion (Coppé et al., 2006). Thus, while cellular senescence may play an initial role in preventing tumorigenesis, a rapid clearing of senescent cells from the intestine may be desirable. *In vivo*, the differentiated epithelial cells turnover rapidly, which may be sufficient to clear the crypt of cells undergoing MMR-induced senescence and reduce the negative consequences of SASP.

On the other hand, long-lasting ISCs undergo apoptosis to immediately eliminate these cells from the body. The choice between apoptosis and senescence may also relate to the levels of DNA damage that can be tolerated by a cell. ISCs may be particularly sensitive to DNA damage, similar to hESCs which undergo rapid apoptosis upon treatment with MNNG (Lin et al., 2014). hESCs are sensitive to DNA damage due to enhanced mitochondrial priming (Liu et al., 2013). This hair-trigger apoptosis mechanism may exist in adult stem cells as well.

The existence of potent MMR-dependent damage responses in intestinal cells suggests that loss of this pathway might provide an immediate selective advantage during the early stages of tumorigenesis in LS patients. ISCs that have lost the remaining wild-type allele of an MMR gene would not be as sensitive to the formation of DNA lesions such as O^6 -MeG, which have been detected in human colons as a result of N-nitroso compounds found in the diet or in cigarette smoke as well as through endogenous bacterial catalysis and nitrosation of amino acids (Povey et al., 2000). The loss of this damage response may tilt the balance in what is normally considered to be a neutral competition between ISCs for residence in the stem cell niche (Lopez-Garcia et al., 2010; Snippert et al., 2010). This would lead to a colonic crypt heavily populated by MMR-defective cells that also harbor a mutator phenotype further accelerating the tumorigenic process. By improving our understanding of the relationship between environmental factors and specific genetic alterations driving tumorigenesis such as loss of MMR, we may gain new insights that will help reduce cancer risk in these patients.

CHAPTER 4

Conclusions and future directions

The DNA MMR pathway maintains genomic stability through the repair of DNA replication errors. Germline mutations in MMR genes lead to the cancer predisposition disease Lynch syndrome. The MMR system is multifaceted. Besides the repair function, MMR can also induce a DNA damage response such as cell cycle arrest and apoptosis to certain forms of DNA damage such as alkylation damage. This MMR-dependent DNA damage response may play an important role in preventing tumorigenesis as well as a response to some chemotherapies in MMR-proficient tumors. Our overall objective was to expand upon our observations of this response in some cancer cell lines and examine the MMR-dependent DNA damage response to alkylation damage in a nontransformed cell model including hPSCs and HIOs which are the most relevant to LS.

A. MMR- dependent DNA damage response in hPSCs

From previous studies using MMR proficient and deficient cancer cell lines, we know that the alkylation agent MNNG induces a MMR-dependent permanent G₂ arrest in cancer cells, with cells only arresting in the second cell cycle after MNNG treatment. Interestingly, we saw a very different response in hPSCs treated with MNNG. First, there was massive apoptosis in hPSCs after MNNG treatment without cell cycle arrest suggesting hPSCs are very sensitive to alkylation damage. This apoptotic response was

shown to be a MMR-dependent response. It is not surprising that hPSCs employ extensive mechanisms including MMR to deal with DNA damage to make sure there is a low tolerance of any damage or mutations accumulated which could be detrimental to development. Besides alkylation damage, hPSCs are also very sensitive to other DNA damaging agents such as gamma-irradiation, UV irradiation and etoposide (Grandela, 2007; Momcilovic et al., 2010; Luo et al., 2012), and prone to apoptosis due to enhanced mitochondrial priming (Liu et al., 2013). This seems to be a unique property of hPSCs and may be the common downstream effect of various forms of DNA damage.

Second, the timing of the response is also very different. Surprisingly, the apoptosis in hPSCs was triggered by MNNG treatment in the first S-phase, contrary to the well - characterized G₂ arrest in the second cell cycle after treatment in the cancer cells, indicating that the MMR-dependent response to alkylation damage in hPSCs is fundamentally different than in transformed cells. Based on the futile cycle model, MMR processing of ^{Me}G–T mismatches in the first S phase results in persistent unreplicated single strand gaps that are converted to lethal double strand breaks (DSBs) in the second S phase. It is the DSBs generated in the second S phase that leads to G₂/M arrest and, eventually, cell death in cancer cells. Thus, transformed cells must have mechanisms to cope with the unreplicated single strand gaps generated in the first S-phase by MMR processing in order to progress into the second cell cycle. These mechanisms have been poorly understood. Evidence has shown that 53BP1 foci may mark unresolved or broken unreplicated single strand gaps that are shielded for repair in the subsequent G₁ or S-phase of the cell cycle using a process that involves the BLM

helicase for resolution (Mankouri, 2013). However, unlike somatic cells, hPSCs do not seem to be able to tolerate perturbed S-phase progression likely caused by MMR processing of the ^{Me}G–T lesions, leading to immediate apoptosis. It will require further investigation to determine why hPSCs fail to stabilize and finish the first S-phase similar to cancer cells. It will be interesting to test whether pathways including 53BP1 and BLM are activated in hPSCs to cope with the unreplicated single strand gaps, whether other more lethal lesions such as DSBs are generated in the first S phase to cause apoptosis, whether the replication stress is so overwhelming that replication forks are collapsing beyond repair. Co-localization assays of BrdU labeled single strand DNA gaps with potential proteins involved in the process may be helpful. Single molecule DNA tracing experiments may be able to help visualize DSBs and collapsed fork structures.

One possible reason that hPSCs might not be able to stabilize the replication in the first S-phase is that hPSCs lack intra-S phase checkpoints that respond to replication stress which would normally function to stabilize replication forks and allow for replication re-start. Indeed, we found that PSCs failed to activate Chk1 in response to MNNG, thus missing a possibly important signaling pathway by which cancer cells survive in the first S-phase. It will be interesting to further investigate why Chk1 is not activated in hPSCs after MNNG treatment even though the upstream kinases ATM/ATR were found to be activated in hPSCs in response to MNNG.

Alternatively, MMR proteins may be functioning through a direct signaling mechanism to recruit stress response proteins to the sites of damage which does not require rounds of

lesion processing to trigger apoptosis. We have shown that MNNG results in the phosphorylation of ATM and ATR as well as the MMR-dependent stabilization and activation of p53, which leads to cell death during the first S phase in hPSCs. Because the balance of pro- and anti-apoptotic proteins in hPSCs due to enhanced mitochondria readiness is such that they are more prone to undergo apoptosis compared to differentiated cells, a low threshold of p53 level is needed to trigger apoptosis in hPSCs. However, the direct signaling and futile cycle mechanisms may not be exclusive and may even contribute simultaneously to trigger rapid apoptosis in hPSCs after MNNG treatment.

B. MMR- dependent DNA damage response in HIOs

The completely different MMR- dependent DNA damage response to MNNG treatment in hPSCs compared to the established response found in cancer cell lines is very interesting, and may be partly cell specific to the hPSCs. To expand on this study, we want to know what the response to alkylation damage is in human intestinal cells and how that may be implicated in Lynch syndrome tumorigenesis. Thus, we used both hESCs-derived and patient-derived HIOs, and found that intestinal cells undergo not only apoptosis, but also a novel senescence response and accelerated differentiation in a MMR-dependent manner following alkylation damage. All these mechanisms can have tumor suppression effects by either eliminating or stopping the proliferation of damaged cells. Thus, loss of MMR function in the intestinal crypts may provide a selective survival advantage that contributes to tumorigenesis particularly in the context

of increased DNA damage. The environment in the colon with N-nitroso carcinogens from diet and bacterial metabolism may contribute to a selective pressure on the cells.

We also found that the cells undergoing apoptosis are primarily the intestinal stem cells suggesting different cell types in the intestine have different responses to damage. The choice between an apoptotic or senescent response may relate to the levels of DNA damage that can be tolerated by a cell. However, the mechanisms of how cells make those choices remain largely unknown because many of the same signaling pathways (such as ATM, ATR, p53 etc) are activated due to DNA damage, yet resulting in different outcomes in the end. It would be very interesting to understand where the divergence is and what controls the pathway choice. There might be cell type specific regulations of the signaling pathways. ISCs may be particularly sensitive to DNA damage, similar to hESCs which undergo rapid apoptosis upon treatment with MNNG. The mitochondria priming mechanism that makes hESCs prone to apoptosis may also exist in ISCs.

All the cells in Lynch syndrome patients are heterozygous in one of the MMR genes and they have intact MMR functions, until one cell loses the other wild type allele and becomes MMR deficient at some point in the patient's lifetime. Those MMR deficient cells could potentially become cancer cells. Thus, it could be a preventive strategy if a potential compound can be found to selectively kill MMR deficient normal (noncancerous) cells and spare the surrounding majority of MMR proficient cells in young LS patients before they actually develop any tumor. Killing MMR deficient normal

cells might be easier to achieve and pose less harm to the rest of the body than killing MMR deficient cancer cells after a tumor has developed in LS patients. For this strategy, HIOs can serve as a great model to screen selective killing compounds on normal human intestinal tissue by comparing WT and MMR deficient HIOs. In addition, HIOs containing specific MMR gene mutations can be used to study how a specific mutation can affect MMR function including the DNA damage response in the intestinal cells providing a functional screen that is more physiologically relevant to LS than functional studies in vitro or in two-dimensional cancer cell lines.

In summary, this study has investigated the MMR-dependent DNA damage response to alkylation damage in hPSCs and HIOs. The response may lead to different outcomes in different cell types and the mechanisms may also vary, but overall the MMR-dependent DNA damage response likely has a tumor suppression effect. Our results raise the possibility that loss of MMR in LS may lead to loss of this protective mechanism in early stage of tumorigenesis and allow MMR deficient cells to have a survival advantage while accumulating mutations that ultimately result in cancer (Figure 4-1).

Figure 4-1.

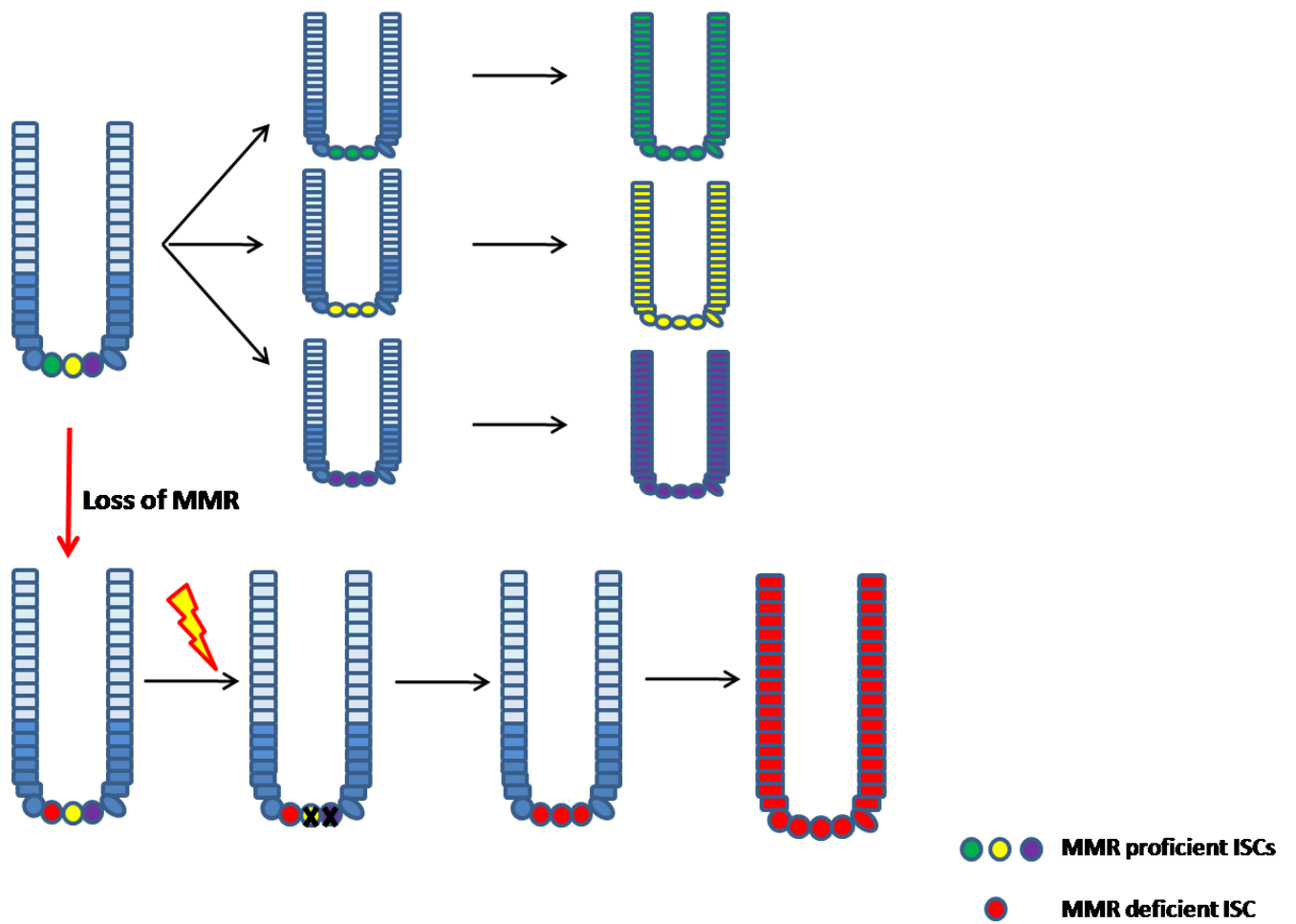


Figure 4-1. MMR deficient ISCs gain survival advantage to populate crypts.

Normally, ISCs at the bottom of a crypt proliferate and compete for the stem cell niche. One of the ISCs will win and occupy the niche, then its descendants will further populate the whole crypt. This process is random, each ISC has the equal chance to win (upper). However, when one of the ISCs loses MMR, the balance is shifted. When encountering certain DNA damage, the MMR proficient ISCs will have a MMR-dependent DNA damage response leading to apoptosis, while MMR deficient ISC can survive to take over the niche and populate the crypt (lower). Now the MMR deficient ISCs will always have better chance to populate the crypts and those crypts are potentially in danger of becoming cancer.

REFERENCES:

- Acosta, J.C., Banito, A., Wuestefeld, T., Georgilis, A., Janich, P., Morton, J.P., Athineos, D., Kang, T.-W., Lasitschka, F., Andrulis, M., *et al.* (2013). A complex secretory program orchestrated by the inflammasome controls paracrine senescence. *Nat Cell Biol* 15, 978-990.
- Adams, B. R., Golding, S. E., Rao, R. R., and Valerie, K. (2010) Dynamic Dependence on ATR and ATM for Double-Strand Break Repair in Human Embryonic Stem Cells and Neural Descendants. *PLoS ONE* 5, e10001.
- Adamson, A., Beardsley, D., Kim, W., Gao, Y., Baskaran, R., and Brown, K. (2005) Methylator-induced, Mismatch Repair-dependent G2 Arrest Is Activated through Chk1 and Chk2. *Mol Biol Cell* 16, 1513-1526.
- Baker D.J., Wijshake T., Tchkonja T., LeBrasseur N.K., Childs B.G., van de Sluis B., Kirkland J.L., van Deursen J.M. (2011). Clearance of p16Ink4a-positive senescent cells delays ageing-associated disorders. *Nature*. 479(7372):232–236.
- Bakkenist, C. J., and Kastan, M. B. (2003) DNA damage activates ATM through intermolecular autophosphorylation and dimer dissociation. *Nature* 421, 499-507.
- Banin, S., Moyal, L., Shieh, S.-Y., Taya, Y., Anderson, C. W., Chessa, L., Smorodinsky, N. I., Prives, C., Reiss, Y., Shiloh, Y., and Ziv, Y. (1998) Enhanced Phosphorylation of p53 by ATM in Response to DNA Damage. *Science* 281, 1674-1677.
- Barker, N. (2014). Adult intestinal stem cells: critical drivers of epithelial homeostasis and regeneration. *Nature Reviews Molecular Cell Biology* 15, 19–33.
- Barker, N., van Es, J.H., Kuipers, J., Kujala, P., van den Born, M., Cozijnsen, M., Haegebarth, A., Korving, J., Begthel, H., Peters, P.J., *et al.* (2007). Identification of stem cells in small intestine and colon by marker gene Lgr5. *449*, 1003-1007.
- Bavik, C., Coleman, I., Dean, J.P., Knudsen, B., Plymate, S., and Nelson, P.S. (2006). The Gene Expression Program of Prostate Fibroblast Senescence Modulates Neoplastic Epithelial Cell Proliferation through Paracrine Mechanisms. *Cancer Res* 66, 794-802.
- Braig M., Schmitt C.A. (2006). Oncogene-induced senescence: putting the brakes on tumor development. *Cancer Res.* 66(6):2881–2884.
- Branzei, D., and Foiani, M. (2009) The checkpoint response to replication stress. *DNA Repair* 8, 1038-1046

Campisi J. (2001). Cellular senescence as a tumor-suppressormechanism. *Trends Cell Biol.* 11(11):S27–S31.

Campisi J., d'Adda di Fagagna F.(2007). Cellular senescence: when bad things happen to good cells. *Nat Rev Mol Cell Biol.* 8(9):729-40.

Canman, C. E., Lim, D.-S., Cimprich, K. A., Taya, Y., Tamai, K., Sakaguchi, K., Appella, E., Kastan, M. B., and Siliciano, J. D. (1998) Activation of the ATM Kinase by Ionizing Radiation and Phosphorylation of p53. *Science* 281, 1677-1679.

Cao, L., Gibson, J.D., Miyamoto, S., Sail, V., Verma, R., Rosenberg, D.W., Nelson, C.E., and Giardina, C. (2011). Intestinal lineage commitment of embryonic stem cells. *Differentiation* 81, 1-10.

Cejka, P., Marra, G., Hemmerle, C., Cannavo, E., Storchova, Z., and Jiricny, J. (2003a) Differential Killing of Mismatch Repair-Deficient and -Proficient Cells: Towards the Therapy of Tumors with Microsatellite Instability. *Cancer Res* 63, 8113-8117.

Cejka, P., Stojic, L., Mojas, N., Russell, A. M., Heinimann, K., Cannavo, E., di Pietro, M., Marra, G., and Jiricny, J. (2003b) Methylation-induced G2/M arrest requires a full complement of the mismatch repair protein hMLH1. *EMBO J.* 22, 2245-2254.

Childs B.G., Durik M., Baker D.J., van Deursen J.M. (2015). Cellular senescence in aging and age-related disease: from mechanisms to therapy. *Nature Medicine.* 21 (12): 1424–1435.

Chung H.Y.Cesari M., Anton S., Marzetti E., Giovannini S., Seo A.Y., Carter C., Yu B.P., Leeuwenburgh C. (2009). Molecular inflammation: underpinnings of aging and age-related diseases. *Ageing Res Rev.* 8(1):18–30.

Constantin, N., Dzantiev, L., Kadyrov, F.A., and Modrich, P. (2005). Human mismatch repair: reconstitution of a nick-directed bidirectional reaction. *J Biol Chem* 280, 39752-39761.

Coppé, J.-P., Kauser, K., Campisi, J., and Beauséjour, C.M. (2006). Secretion of Vascular Endothelial Growth Factor by Primary Human Fibroblasts at Senescence. *J BiolChem* 281, 29568-29574.

Desmarais, J. A., Hoffmann, M. J., Bingham, G., Gagou, M. E., Meuth, M., and Andrews, P. W. (2012) Human Embryonic Stem Cells Fail to Activate CHK1 and Commit to Apoptosis in Response to DNA Replication Stress. *Stem Cells* 30, 1385-1393.

Dietmaier, W., Wallinger, S., Bocker, T., Kullmann, F., Fishel, R., and Ruschoff, J. (1997) Diagnostic microsatellite instability: definition and correlation with mismatch repair protein expression. *Cancer Res* 57, 4749-4756.

Duckett, D. R., Drummond, J. T., Murchie, A. I., Reardon, J. T., Sancar, A., Lilley, D. M., and Modrich, P. (1996). Human MutS α recognizes damaged DNA base pairs containing O⁶-methylguanine, O⁴-methylthymine, or the cisplatin d(GpG) adduct. *Proc Natl Acad Sci U S A* 93, 6443-6447.

Duval, A., and Hamelin, R. (2002). Mutations at coding repeat sequences in mismatch repair-deficient human cancers: toward a new concept of target genes for instability. *Cancer Res* 62, 2447-2454.

Fan, J., Robert, C., Jang, Y. Y., Liu, H., Sharkis, S., Baylin, S. B., and Rassool, F. V. (2011) Human induced pluripotent cells resemble embryonic stem cells demonstrating enhanced levels of DNA repair and efficacy of nonhomologous end-joining. *Mutat Res* 713, 8-17.

Filion, T. M., Qiao, M., Ghule, P. N., Mandeville, M., van Wijnen, A. J., Stein, J. L., Lian, J. B., Altieri, D. C., and Stein, G. S. (2009) Survival responses of human embryonic stem cells to DNA damage. *J Cell Phys* 220, 586-592.

Finkbeiner, Stacy R., Hill, David R., Altheim, Christopher H., Dedhia, Priya H., Taylor, Matthew J., Tsai, Y.-H., Chin, Alana M., Mahe, Maxime M., Watson, Carey L., Freeman, Jennifer J., *et al.* (2015). Transcriptome-wide Analysis Reveals Hallmarks of Human Intestine Development and Maturation In Vitro and In Vivo. *Stem Cell Reports* 4, 1140-1155.

Fishel, R., and Kolodner, R. D. (1995) Identification of mismatch repair genes and their role in the development of cancer. *Curr Opin Genet Dev* 5, 382-395.

Fishel, R., and Wilson, T. (1997). MutS homologs in mammalian cells. *Curr Opin Genet Dev* 7, 105-113.

Fung, H., and Weinstock, D. M. (2011) Repair at Single Targeted DNA Double-Strand Breaks in Pluripotent and Differentiated Human Cells. *PLoS ONE* 6, e20514.

Gerson, S. L. (2004). MGMT: its role in cancer aetiology and cancer therapeutics, In *Nat Rev Cancer*, pp. 296-307.

Goldmacher, V. S., Cuzick, R. A., Jr., and Thilly, W. G. (1986). Isolation and partial characterization of human cell mutants differing in sensitivity to killing and mutation by methyl nitrosourea and N-methyl-N'-nitro-N-nitrosoguanidine. *J Biol Chem* 267, 12462-12471.

Grandela, C., Pera, M. F., and Wolvetang, E. J. (2007) p53 is required for etoposide-induced apoptosis of human embryonic stem cells. *Stem Cell Res* 1, 116-128.

Guerra C., Collado M., Navas C., Schuhmacher A.J., Hernández-Porras I., Cañamero M., Rodríguez-Justo M., Serrano M., Barbacid M. (2011). Pancreatitis-induced

inflammation contributes to pancreatic cancer by inhibiting oncogene-induced senescence. *Cancer Cell* 19(6):728–739.

Hannan, Nicholas R.F., Fordham, Robert P., Syed, Yasir A., Moignard, V., Berry, A., Bautista, R., Hanley, Neil A., Jensen, Kim B., and Vallier, L. (2013). Generation of Multipotent Foregut Stem Cells from Human Pluripotent Stem Cells. *Stem Cell Reports* 1, 293-306.

Harfe, B. D. and Jinks-Robertson, S. (2000). DNA mismatch repair and genetic instability. *Annu. Rev. Genet.* 34, 359–399.

Harrigan, J. A., Belotserkovskaya, R., Coates, J., Dimitrova, D. S., Polo, S. E., Bradshaw, C. R., Fraser, P., and Jackson, S. P. (2011) Replication stress induces 53BP1-containing OPT domains in G1 cells. *J Cell Biol* 193, 97-108.

Heinen, C. D., Schmutte, C., and Fishel, R. (2002) DNA Repair and Tumorigenesis: Lessons from Hereditary Cancer Syndromes. *Can Biol Ther* 1, 477-485.

Hickman, M. J., and Samson, L. D. (2004). Apoptotic signaling in response to a single type of DNA lesion, O(6)-methylguanine. *Mol Cell* 14, 105-116.

Hsieh, P., and Yamane, K. (2008). DNA mismatch repair: molecular mechanism, cancer, and ageing. *Mech Ageing Dev* 729, 391-407.

Jiricny, J. (2006). MutLalpha: at the cutting edge of mismatch repair. *Cell* 126,239-241.

Kaina, B., Ziouta, A., Ochs, K., and Coquerelle, T. (1997) Chromosomal instability, reproductive cell death and apoptosis induced by O6-methylguanine in Mex-, Mex+ and methylation-tolerant mismatch repair compromised cells: facts and models. *Mutat Res* 381, 227-241.

Kane, M., Loda, M., Gaida, G., Lipman, J., Mishra, R., Goldman, H., Jessup, J., and Kolodner, R. (1997) Methylation of the hMLH1 promoter correlates with lack of expression of hMLH1 in sporadic colon tumors and mismatch repair-defective human tumor cell lines. *Cancer Res* 57, 808-811.

Kang, T.-W., Yevsa, T., Woller, N., Hoenicke, L., Wuestefeld, T., Dauch, D., Hohmeyer, A., Gereke, M., Rudalska, R., Potapova, A., *et al.* (2011). Senescence surveillance of pre-malignant hepatocytes limits liver cancer development. *Nature* 479, 547-551.

Karran, P. (2001). Mechanisms of tolerance to DNA damaging therapeutic drugs. *Carcinogenesis* 22, 1931-1937.

Kolodner, R. (1996). Biochemistry and genetics of eukaryotic mismatch repair. *Genes Dev* 10, 1433-1442.

Kolodner, R. D., and Marsischky, G. T. (1999) Eukaryotic DNA mismatch repair. *Curr Opin Genet Dev* 9, 89-96.

Krtolica, A., Parrinello, S., Lockett, S., Desprez, P.-Y., and Campisi, J. (2001). Senescent fibroblasts promote epithelial cell growth and tumorigenesis: A link between cancer and aging. *Proc Natl Acad Sci USA* 98, 12072-12077.

Kunkel, T. A., and Erie, D. A. (2005) DNA MISMATCH REPAIR. *Ann Rev Biochem* 74, 681- 710.

Lahue, R. S., Au, K. G., and Modrich, P. (1989). DNA mismatch correction in a defined system. *Science* 245, 160-164.

Li, G. M. (2008). Mechanisms and functions of DNA mismatch repair. *Cell Res* 18, 85-98.

Li, Z., Pearlman, A.H., and Hsieh, P. (2016). DNA mismatch repair and the DNA damage response. *DNA Repair* 38, 94-101.

Lin, B., Gupta, D., and Heinen, C.D. (2014). Human Pluripotent Stem Cells Have a Novel Mismatch Repair-dependent Damage Response. *J Biol Chem* 289, 24314-24324.

Lin, D. P., Wang, Y., Scherer, S. J., Clark, A. B., Yang, K., Avdievich, E., Jin, B., Werling, U., Parris, T., Kurihara, N., et al. (2004). An Msh2 point mutation uncouples DNA mismatch repair and apoptosis. *Cancer Res* 64, 517-522.

Liu, S., Shiotani, B., Lahiri, M., Maréchal, A., Tse, A., Leung, Charles Chung Y., Glover, J. N. M., Yang, Xiaohong H., and Zou, L. (2011) ATR Autophosphorylation as a Molecular Switch for Checkpoint Activation. *Mol Cell* 43, 192-202.

Liu, Y., Fang, Y., Shao, H., Lindsey-Boltz, L., Sancar, A., and Modrich, P. (2010) Interactions of Human Mismatch Repair Proteins MutS and MutL with Proteins of the ATR-Chk1 Pathway. *J Biol Chem* 285, 5974-5982.

Liu, Julia C., Guan, X., Ryan, Jeremy A., Rivera, Ana G., Mock, C., Agarwal, V., Letai, A., Lerou, Paul H., and Lahav, G. (2013) High Mitochondrial Priming Sensitizes hESCs to DNA Damage-Induced Apoptosis. *Cell Stem Cell* 13, 483-491.

Loeb, L. A., Springgate, C. F., and Battula, N. (1974). Errors in DNA replication as a basis of malignant changes. *Cancer Res* 34, 2311-2321.

Lopez-Garcia, C., Klein, A.M., Simons, B.D., and Winton, D.J. (2010). Intestinal Stem Cell Replacement Follows a Pattern of Neutral Drift. *Science* 330, 822-825.

Lukas, C., Savic, V., Bekker-Jensen, S., Doil, C., Neumann, B., Solvhoj Pedersen, R., Grofte, M., Chan, K. L., Hickson, I. D., Bartek, J., and Lukas, J. (2011) 53BP1 nuclear bodies form around DNA lesions generated by mitotic transmission of chromosomes under replication stress. *Nat Cell Biol* 13, 243-253.

Luo, L. Z., Gopalakrishna-Pillai, S., Nay, S. L., Park, S.-W., Bates, S. E., Zeng, X., Iverson, L. E., and O'Connor, T. R. (2012) DNA Repair in Human Pluripotent Stem Cells Is Distinct from That in Non-Pluripotent Human Cells. *PLoS ONE* 7, e30541.

Lynch, H., Lynch, P., Lanspa, S., Snyder, C., Lynch, J., and Boland, C. (2009) Review of the Lynch syndrome: history, molecular genetics, screening, differential diagnosis, and medicolegal ramifications. *Clini Genet* 76, 1-18.

Lynch, H.T., Snyder, C.L., Shaw, T.G., Heinen, C.D., and Hitchins, M.P. (2015). Milestones of Lynch syndrome: 1895-2015. *Nat Rev Cancer* 15, 181-194.

Mankouri, H. W., Huttner, D., and Hickson, I. D. (2013) How unfinished business from S-phase affects mitosis and beyond. *EMBO J* 32, 2661-2671.

Martin A. and Scharff M. (2002). AID and mismatch repair in antibody diversification. *Nature Reviews Immunology* 2, 605-614.

Mastrocola, A. S., and Heinen, C. D. (2010a) Lynch syndrome-associated mutations in MSH2 alter DNA repair and checkpoint response functions in vivo. *Hum Mutat* 31, E1699-E1708.

Mastrocola, A. S., and Heinen, C. D. (2010b). Nuclear reorganization of DNA mismatch repair proteins in response to DNA damage. *DNA Repair (Amst)* 9, 120-133.

Maynard, S., Swistowska, A. M., Lee, J. W., Liu, Y., Liu, S.-T., Da Cruz, A. B., Rao, M., de Souza-Pinto, N. C., Zeng, X., and Bohr, V. A. (2008) Human Embryonic Stem Cells Have Enhanced Repair of Multiple Forms of DNA Damage. *Stem Cells* 26, 2266-2274.

McCracken, K.W., Cata, E.M., Crawford, C.M., Sinagoga, K.L., Schumacher, M., Rockich, B.E., Tsai, Y.-H., Mayhew, C.N., Spence, J.R., Zavros, Y., *et al.* (2014). Modelling human development and disease in pluripotent stem-cell-derived gastric organoids. *Nature* 516, 400-404.

McCracken, K.W., Howell, J.C., Wells, J.M., and Spence, J.R. (2011). Generating human intestinal tissue from pluripotent stem cells in vitro. *Nat Protocols* 6, 1920-1928.

Modrich, P. (1991). Mechanisms and Biological Effects of Mismatch Repair. *Ann Rev Gen* 25, 229-253.

Modrich, P. (2006) Mechanisms in eukaryotic mismatch repair. *J. Biol. Chem.* 281, 30305-30309.

Momcilovic, O., Knobloch, L., Fornasaglio, J., Varum, S., Easley, C., and Schatten, G. (2010) DNA Damage Responses in Human Induced Pluripotent Stem Cells and Embryonic Stem Cells. *PLoS ONE* 5, e13410.

Noonan, E. M., Shah, D., Yaffe, M. B., Lauffenburger, D. A., and Samson, L. D. (2012) O⁶- Methylguanine DNA lesions induce an intra-S-phase arrest from which cells exit into apoptosis governed by early and late multi-pathway signaling network activation. *Integrat Biol* 4, 1237- 1255.

Poulogiannis, G., Frayling, I.M., and Arends, M.J. (2010). DNA mismatch repair deficiency in sporadic colorectal cancer and Lynch syndrome. In *Histopathology*, pp. 167-179.

Povey, A.C., Hall, C.N., Badawi, A.F., Cooper, D.P., and O'Connor, P.J. (2000). Elevated levels of the pro-carcinogenic adduct, O6-methylguanine, in normal DNA from the cancer prone regions of the large bowel. *Gut* 47, 362-365.

Prieur A., Peeper D.S. (2008). Cellular senescence in vivo: a barrier to tumorigenesis. *Curr Opin Cell Biol.* 20(2):150–155.

Qin, H., Yu, T., Qing, T., Liu, Y., Zhao, Y., Cai, J., Li, J., Song, Z., Qu, X., Zhou, P., Wu, J., Ding, M., and Deng, H. (2007) Regulation of Apoptosis and Differentiation by p53 in Human Embryonic Stem Cells. *J Biol Chem* 282, 5842-5852.

Rajesh, P., Rajesh, C., Wyatt, M. D., and Pittman, D. L. (2010) RAD51D protects against MLH1- dependent cytotoxic responses to O6-methylguanine. *DNA Repair* 9, 458-467.

Ricciardiello, L., Ahnen, D.J., and Lynch, P.M. (2016). Chemoprevention of hereditary colon cancers: time for new strategies. *Nat Rev Gastroenterol Hepatol* 13, 352-361.

Sato, T., Stange, D.E., Ferrante, M., Vries, R.G.J., van Es, J.H., van den Brink, S., van Houdt, W.J., Pronk, A., van Gorp, J., Siersema, P.D., et al. (2011). Long-term Expansion of Epithelial Organoids From Human Colon, Adenoma, Adenocarcinoma, and Barrett's Epithelium. *Gastroenterology* 141, 1762-1772.

Sirbu, B. M., Couch, F. B., Feigerle, J. T., Bhaskara, S., Hiebert, S. W., and Cortez, D. (2011) Analysis of protein dynamics at active, stalled, and collapsed replication forks. *Genes Devel* 25, 1320-1327.

Snippert, H.J., van der Flier, L.G., Sato, T., van Es, J.H., van den Born, M., Kroon-Veenboer, C., Barker, N., Klein, A.M., van Rheenen, J., Simons, B.D., et al. (2010).

Intestinal Crypt Homeostasis Results from Neutral Competition between Symmetrically Dividing Lgr5 Stem Cells. *Cell* 143, 134-144.

Sparmann A, Bar-Sagi D. (2004). Ras-induced interleukin-8 expression plays a critical role in tumor growth and angiogenesis. *Cancer Cell*. 6(5):447–458.

Spence, J.R., Mayhew, C.N., Rankin, S.A., Kuhar, M.F., Vallance, J.E., Tolle, K., Hoskins, E.E., Kalinichenko, V.V., Wells, S.I., Zorn, A.M., et al. (2011). Directed differentiation of human pluripotent stem cells into intestinal tissue in vitro. *Nature* 470, 105-109.

Stojic, L., Brun, R., and Jiricny, J. (2004a). Mismatch repair and DNA damage signalling. *DNA Repair (Amst)* 3, 1091-1101.

Stojic, L., Mojas, N., Cejka, P., Di Pietro, M., Ferrari, S., Marra, G., and Jiricny, J. (2004b). Mismatch repair-dependent G2 checkpoint induced by low doses of SN1 type methylating agents requires the ATR kinase. *Genes Dev* 18, 1331-1344.

Strand, M., Prolla, T.A., Liskay, R.M., and Petes, T.D. (1993). Destabilization of tracts of simple repetitive DNA in yeast by mutations affecting DNA mismatch repair *Nature* 365, 274-276.

Tajima, A., Hess, M.T., Cabrera, B.L., Kolodner, R.D., and Carethers, J.M. (2004). The mismatch repair complex hMutS alpha recognizes 5-fluorouracil-modified DNA: implications for chemosensitivity and resistance. *Gastroenterology* 127, 1678-1684.

Tamm I, Kikuchi T, Cardinale I, Krueger JG.(1994). Cell-adhesion-disrupting action of interleukin 6 in human ductal breast carcinoma cells. *Proc Natl Acad Sci U S A*. 91(8):3329–3333.

Tibbetts, R. S., Brumbaugh, K. M., Williams, J. M., Sarkaria, J. N., Cliby, W. A., Shieh, S. Y., Taya, Y., Prives, C., and Abraham, R. T. (1999) A role for ATR in the DNA damage-induced phosphorylation of p53. *Genes Dev* 13, 152-157.

Vasen, H.F.A., Moslein, G., Alonso, A., Bernstein, I., Bertario, L., Blanco, I., Burn, J., Capella, G., Engel, C., Frayling, I. (2007). Guidelines for the clinical management of Lynch syndrome. In *J Med Genet*, pp 353-362.

Venkatesan, R. N., Hsu, J. J., Lawrence, N. A., Preston, B. D., and Loeb, L. A. (2006) Mutator Phenotypes Caused by Substitution at a Conserved Motif A Residue in Eukaryotic DNA Polymerase delta. *J Biol Chem* 281, 4486-4494.

Wang, Y., and Qin, J. (2003) MSH2 and ATR form a signaling module and regulate two branches of the damage response to DNA methylation. *Proc Natl Acad Sci U S A* 100, 15387-15392.

Wang, F., Scoville, D., He, X.C., Mahe, M.M., Box, A., Perry, J.M., Smith, N.R., Lei, N.Y., Davies, P.S., Fuller, M.K., *et al.* (2013). Isolation and Characterization of Intestinal Stem Cells Based on Surface Marker Combinations and Colony-Formation Assay. *Gastroenterology* 145, 383-395.e321.

White, A.C., and Lowry, W.E. (2015). Refining the role for adult stem cells as cancer cells of origin. *Trends in Cell Biology* 25, 11-20.

Wilson, K. D., Sun, N., Huang, M., Zhang, W. Y., Lee, A. S., Li, Z., Wang, S. X., and Wu, J. C. (2010) Effects of Ionizing Radiation on Self-Renewal and Pluripotency of Human Embryonic Stem Cells. *Cancer Res* 70, 5539-5548.

Xue W., Zender L., Miething C., Dickins R.A., Hernando E., Krizhanovsky V., Cordon-Cardo C., Lowe S.W. (2007). Senescence and tumour clearance is triggered by p53 restoration in murine liver carcinomas. *Nature*. 445(7128):656–660.

Yang, G., Scherer, S. J., Shell, S. S., Yang, K., Kim, M., Lipkin, M., Kucherlapati, R., Kolodner, R. D., and Edelmann, W. (2004). Dominant effects of an Msh6 missense mutation on DNA repair and cancer susceptibility. *Cancer Cell* 6, 139-150.

Yin, X., Farin, H.F., van Es, J.H., Clevers, H., Langer, R., and Karp, J.M. (2014). Niche-independent high-purity cultures of Lgr5+ intestinal stem cells and their progeny. *Nat Meth* 11, 106-112.

York, S. J., and Modrich, P. (2006). Mismatch repair-dependent iterative excision at irreparable O6-methylguanine lesions in human nuclear extracts. *J Biol Chem* 281, 22674-22683.

Yoshioka, K., Yoshioka, Y., and Hsieh, P. (2006) ATR Kinase Activation Mediated by MutSa and MutLa in Response to Cytotoxic O6-Methylguanine Adducts. *Mol Cell* 22, 501-510.

Zeng, H., Guo, M., Martins-Taylor, K., Wang, X., Zhang, Z., Park, J. W., Zhan, S., Kronenberg, M. S., Lichtler, A., Liu, H.-X., Chen, F.-P., Yue, L., Li, X.-J., and Xu, R.-H. (2010) Specification of Region-Specific Neurons Including Forebrain Glutamatergic Neurons from Human Induced Pluripotent Stem Cells. *PLoS ONE* 5, e11853.

Zhang, H., Richards, B., Wilson, T., Lloyd, M., Cranston, A., Thorburn, A., Fishel, R., and Meuth, M. (1999) Apoptosis induced by overexpression of hMSH2 or hMLH1. *Cancer Res* 59, 3021-3027.

Zhang, Y., Yuan, F., Presnell, S.R., Tian, K., Gao, Y., Tomkinson, A.E., Gu, L., and Li, G.M. (2005). Reconstitution of 5'-directed human mismatch repair in a purified system. *Cell* 122, 693-705.

Zhou, B., Huang, C., Yang, J., Lu, J., Dong, Q., and Sun, L. Z. (2009) Preparation of heteroduplex EGFP plasmid for in vivo mismatch repair activity assay. *Anal Biochem* 1, 167-169.